EarthCARE   - Earth Clouds, Aerosols and Radiation Explorer
SPECTRA   - Surface Processes and Ecosystem Changes Through Response Analysis
WALES   - Water Vapour Lidar Experiment in Space
ACE+   - Atmosphere and Climate Explorer
EGPM   - European Contribution to Global Precipitation Measurement
Swarm   - The Earth's Magnetic Field and Environment Explorers

European Space Agency
Agence spatiale européenne

REPORTS FOR MISSION SELECTION
THE SIX CANDIDATE EARTH EXPLORER MISSIONS

REPORTS FOR MISSION SELECTION
THE SIX CANDIDATE EARTH EXPLORER MISSIONS

EarthCARE –
Earth Clouds, Aerosols and Radiation Explorer

Contents

1. Introduction

The ESA Living Planet Programme includes two types of complementary user driven missions: the research-oriented Earth Explorer missions and the operational service oriented Earth Watch missions. These missions are implemented through the Earth Observation Envelope Programme (EOEP) and the Earth Watch Programme, where the Earth Explorer missions are completely covered by the EOEP.

Earth Explorer missions are divided into two classes, with Core missions being larger missions addressing complex issues of wide scientific interest, and Opportunity missions, which are smaller in terms of cost to ESA and address more limited issues. Both types of missions address the research objectives set out in the Living Planet Programme document (ESA SP-1227 1998), which describes the plans for the Agency's strategy for Earth Observation in the post-2000 time frame. All Earth Explorer missions are proposed, defined, evaluated and recommended by the scientific community.

Following a call for Core mission ideas in 2000 and selection of five of the ten proposals for pre-feasibility study, three of the candidates, EarthCARE, SPECTRA and WALES, were chosen for feasibility study in November 2001. In response to a call for Opportunity mission proposals in 2001, which resulted in 25 full proposals being submitted by early 2002, three mission candidates, ACE+, EGPM and SWARM, were also chosen for feasibility study. The Phase-A studies for all six Earth Explorer candidate missions are being finalised by early 2004, forming the basis for the Reports for Mission Selection for all six candidate missions.

This Report for Mission Selection for EarthCARE was prepared based on inputs from the Mission Advisory group (MAG) consisting of A. Ansmann (Institut für Troposphärenforschung, Leipzig, Germany), F. Berger (Technical University, Dresden, Germany), J.-P. Blanchet (UQAM, University of Quebec, Montreal, Canada), D. Donovan (KNMI, De Bilt, The Netherlands), A.J. Illingworth (University of Reading, Reading, UK), R.S. Kandel (LMD, Ecole Polytechnique, Palaiseau, France), H. Kumagai (Communication Research Laboratory, Tokyo, Japan), E. Lopez-Baeza (University of Valencia, Valencia, Spain), M. Miller (ECMWF, Reading, UK), T. Nakajima (CCSR, University of Tokyo, Japan), H. Okamoto (Tohoku University, Sendai, Japan), J. Pelon (Service d'Aeronomie/IPSL, Paris, France), R. Rizzi (University of Bologna, Bologna, Italy) and A. Slingo (University of Reading, Reading, UK). Parts of the Report have been prepared by the Executive based on inputs provided by the industrial Phase-A contractors.

The Report for Mission Selection for EarthCARE, together with those for the other five Earth Explorer candidate missions, is being circulated within the Earth Observation research community in preparation for a User Consultation Meeting at ESRIN, Frascati, Italy, in April 2004.

2. Background and Scientific Justification

2.1 Overview

Difficulties in representing aerosols, clouds, and convection in numerical models of the atmosphere seriously limit the ability to provide accurate weather forecasts and reliable predictions of future climate. These factors govern the radiation balance and hence the temperature of the Earth and are directly responsible for the production of precipitation and thus control the hydrological cycle. In summary:

(a) Aerosols

Aerosols have a direct radiative impact by reflecting solar radiation back to space, which leads to cooling. Absorbing aerosols, e.g. carbon from anthropogenic sources, can lead to local heating. Aerosols also control the radiative properties of clouds and their ability to produce precipitation. The low concentration of aerosol particles in marine air leads to water clouds with a small number of relatively large droplets. In contrast, the high concentration of aerosols in continental and polluted air results in water clouds with a much higher concentration of smaller droplets. Continental clouds therefore not only have a higher albedo and reflect more sunlight back to space, but also are much more stable and long-lived and less likely to produce precipitation. Aerosols also control the glaciation process, yet their effect on the properties of ice clouds is essentially unknown. There is a need to quantify the degree to which aerosols are responsible for the observed rapid reduction in the albedo of freshly fallen snow. Present observations of global aerosol properties are limited to optical depth and a crude estimate of particle size. This is very unsatisfactory, since we need to know their chemical composition, whether they scatter or absorb, and their vertical and geographical distribution.

(b) Clouds

Clouds are the principal modulators of the Earth's radiation balance. Currently, there are global estimates of cloud cover, but little information on their vertical extent or the condensed mass of ice or liquid cloud water. Low clouds cool the climate by reflecting short wave solar radiation back to space, whereas high clouds warm the climate because they are cold and emit less infrared radiation to space. In the present climate, these two effects are large and have opposite signs. Any changes in the vertical distribution of clouds in a future warmer climate could lead to large changes in the net radiative forcing. Climate models disagree as to whether this attenuates or amplifies the effect of the original direct greenhouse gas warming. Uncertainties in the vertical profiles of clouds are largely responsible for the current unacceptable spread in predictions of future global warming, and also limit the accuracy of numerical weather prediction. Models are able to produce the present observed top-of-the-atmosphere

radiation but with very different vertical profiles of clouds and water content. To evaluate models, observations of cloud profiles are urgently required, so that the ability of models to provide reliable weather forecasts and predictions of future global warming can be improved.

(c) Convection and Precipitation Processes

Clouds are the source of all precipitation, but details of this process are poorly understood. At present, models convert cloud condensate in a grid box to precipitation either by slow widespread ascent, or, for the more intense rainfall, by convection. Major difficulties include the large spread in model predictions of cloud condensate, the efficiency with which this is converted to precipitation, and the representation of sub-grid-scale convective motions. The extent to which vigorous tropical convection introduces moisture into the stratosphere is uncertain. It is also known that the modelled diurnal cycle of convection is incorrect. Understanding these processes is crucial for quantitative precipitation forecasting. The societal benefits in providing warning of flash flooding would be immense. Global observations of the probability distribution function of vertical motions within the grid box to constrain convective parameterisation schemes are needed.

2.2 Radiation and the Need for Reliable Models

Whether or not recent global warming is entirely attributable to human activities, there is no reasonable doubt that continuation and acceleration of the already strong anthropogenic alteration of the atmosphere's composition must lead to stronger climate change than was observed in the 20th century (IPCC, 2001). Such change will necessarily involve changes in the distributions of precipitation and runoff, and will modify distributions of events such as violent winter storms, tropical cyclones, extended heat and drought, and flood-producing extreme rainfall.

(a) Radiation

Radiative effects play a governing role in climate, constituting both the source (solar radiation) and the ultimate sink (thermal infrared radiation to space) of energy in the Earth-atmosphere system. Both *aerosols* and *clouds* are major actors in the climate-radiation connection.

(b) Radiative Forcing

For greenhouse gases, anthropogenic alteration of the atmosphere over past decades and centuries is well established. The corresponding radiative forcing can be computed with confidence, e.g. for the year 2000 compared to 1750 (Fig. 2.1). For *aerosols*, however, radiative forcing is poorly understood.
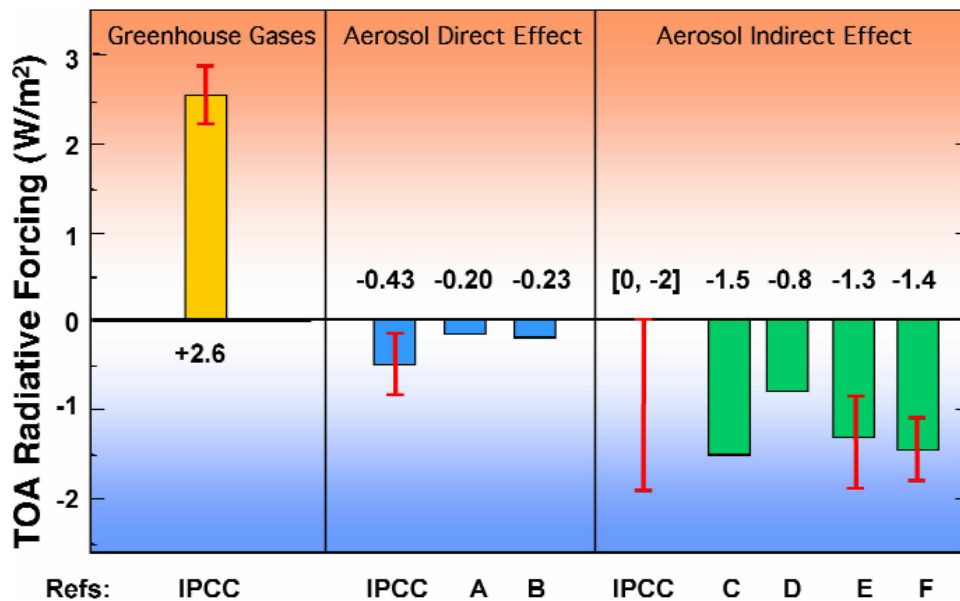
Figure 2.1: *Global annual mean radiative forcing at the top of atmosphere corresponding to changes from 1750 to 2000 following IPCC (2001) together with recent assessments of aerosol direct and indirect effects (modelling and satellite studies). Note that although direct radiative forcing is fairly well known, indirect forcing of aerosols is extremely uncertain. (A: Takemura et al., 2002, B: Kaufman et al., 2003, C: Takemura, 2003a, D: Takemura, 2003b, E: Nakajima et al., 2001, F: Sekiguchi et al., 2003)*

(c) Climate Sensitivity and Feedbacks

For a given emissions scenario (translated into time-dependent radiative forcing), different model simulations exhibit a wide range of global warming. A major factor in these differences is certainly the model's 'water vapour feedback', whose strength depends to a large extent on the parameterisation of the condensation/freezing processes in clouds. These also strongly influence the 'cloud-radiation feedback', for which even the sign is unknown. It is well known that different climate models, providing reasonable simulations of the present climate, give widely different changes (both in magnitude and sign) in their shortwave, longwave, and net cloud radiative forcing for a given scenario. Observations are needed to provide much stricter constraints on the cloud process parameterisations that to a large extent determine the strength of the water vapour and cloud-radiation feedbacks.

(d) Model Needs

Although part of the huge range of global warming projections (viz. from 1.4 to 5.8 K for 2100) arises from the different emission scenarios, a significant range of climate model uncertainty remains. For an individual scenario, in addition to warming ranging from 2 to 4 K, different simulations give inconsistent projections of the changes in

precipitation and runoff in important regions (e.g. eastern North America). This may depend in part on parameterisations of surface water processes, but certainly depends also on precipitation and so on clouds. The shortcomings in the treatment of cloud and aerosol processes in climate models arise from lack of observations to validate cloud and aerosol parameterisation schemes. The same difficulties bedevil numerical weather prediction models used for short and medium range and seasonal forecasting.

2.3   Numerical Weather Prediction and Climate Models

All such models divide the atmosphere into a series of grid boxes, typically around 50 km in the horizontal and 500 m in the vertical. By the time of launch of EarthCARE, numerical weather forecasting models are expected to have horizontal resolutions in the order of 10 to 20 km and up to 90 levels in the vertical. For each box, clouds are represented by prognostic variables such as fractional cloud cover, ice and liquid water content. The radiative transfer in atmospheric models also requires assumptions on cloud overlap for each vertical stack of grid boxes and particle sizes. The overlap assumptions affect both the radiative transfer and the precipitation efficiency of the clouds.

A first step is to evaluate whether the *current* weather and climate is being correctly represented in numerical models to give us more confidence in the climate predictions. Recently Potter and Cess (2004) compared cloud-radiative forcing (CRF) predicted by a group of 19 atmospheric general circulation models. It was has found that CRF at the top-of-the atmosphere predicted by many GCMs shows a significant negative bias where compared to ERBE measurements. This means that GCMs significantly overestimate cloud radiative cooling. Out of the group of 19 model analyses, those that did predict accurate TOA fluxes were found to agree with observations only due to compensating errors in either cloud vertical structure, cloud optical depth or cloud fraction. This clearly highlights the need for better measurements of cloud property vertical profiles on a global basis. Using ISCCP (International Satellite Cloud Climatology Project) cloud data in the AMIP (Atmospheric Model Intercomparison Project) comparisons, it has been shown that 'realistic' models correctly reproducing radiation fluxes at the top of the atmosphere strongly disagree in their assessments of cloud water (Fig. 2.2). Clearly, stronger empirical constraints are needed to narrow this range, in particular measurements of total cloud water over land surfaces, where passive microwave radiometry is inadequate. Vertical cloud water profiles are needed to evaluate the model parameterisations of in-cloud processes and cloud-aerosol-radiation interactions. EarthCARE data products can be compared with GCMs and climate models to identify errors and biases in these models. This should lead to improved parameterisation schemes in the models and consequent improvements in weather forecasts, and more reliable predictions of temperature, precipitation and extreme events in the future climate.
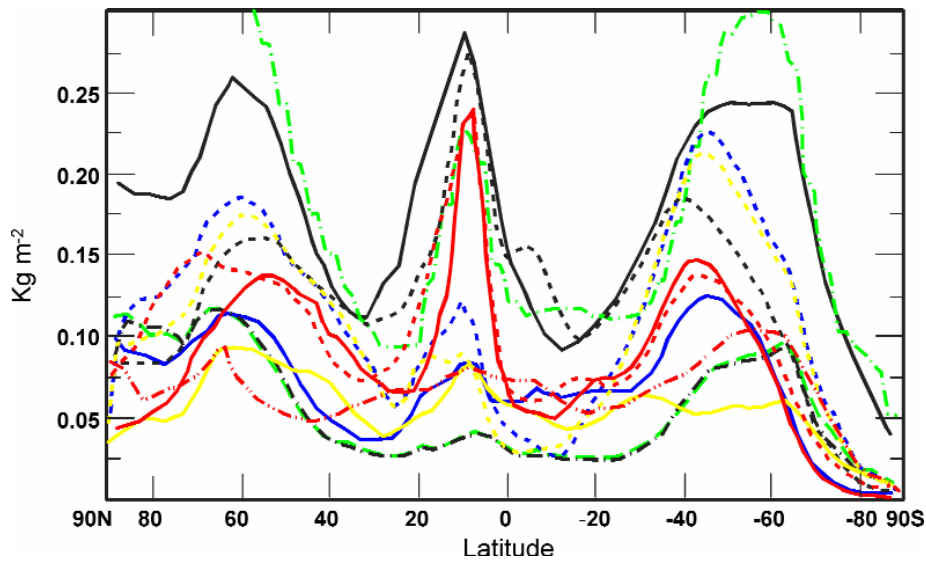
Figure 2.2: *Zonally and vertically integrated cloud water for 14 different AMIP2 climatologies for northern summer. The black curve shows the ECMWF result.*

2.4 Aerosols

Changes in aerosols directly modify solar radiation reaching the ground, and also affect microphysical, biochemical and photochemical processes in the atmosphere including processes affecting cloud properties. In particular, increases in aerosols resulting from human activities have 'indirect' radiative effects by (i) increasing the cloud albedo by decreasing the droplet size, and (ii) changing the cloud lifetime. Indirect aerosol effects could be very important and must be taken into account in global and regional climate change forecasts. An example of the direct and indirect impact of anthropogenic aerosols (biomass burning and ship tracks) can be seen in the MERIS satellite image shown in Figure 2.3. Unlike greenhouse gases, aerosols have short atmospheric residence times, and thus are non-uniformly distributed in space and time, which complicates efforts to account for their effects.

Moreover, the presence of thin aerosol layers, difficult to detect by passive measurements, can induce strong errors in underlying cloud property retrievals. Anthropogenic aerosol and aerosol precursor emissions are likely to vary in time and space over coming decades, and it is essential to develop tools for evaluating to what extent passive measurements can monitor the associated forcing. New active measurements of aerosol profiles are essential.
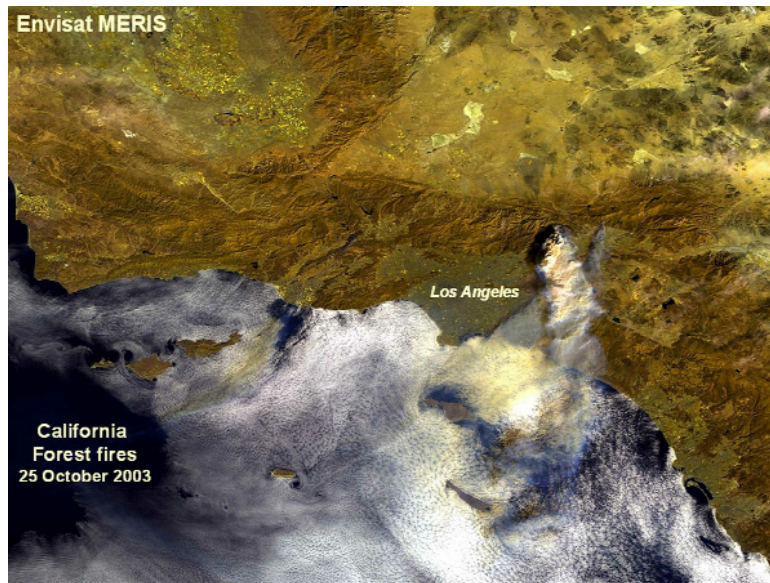
Figure 2.3: Wild fires in California (25 October, 2003, ESA, MERIS). The aerosols are transported SSW and interact with low level cloud off the Californian coast. Aerosols above the stratocumulus cloud layer reduce their reflectivity (positive forcing), while aerosols within the cloud lead to brighter clouds (negative forcing). The same is true for the ship tracks visible in the left part of the image.

2.5 Clouds

In general, low-level clouds cool the Earth by reflecting more sunlight back to space, but high level cold clouds tend to warm the Earth by losing less infrared radiation to space. Hence, if cloud properties change in response to any future climate change, then the 'cloud radiative feedback' can either amplify the original direct radiative forcing or counteract it. Changes in the vertical profile of clouds lead to different heating rates and consequent important changes in the atmospheric dynamics that then feed back to changes in the cloud profiles. Current satellite instruments constrain the total incoming and outgoing radiation at the top of the atmosphere, but cannot provide sufficiently accurate determinations of cloud profiles and consequent energy heating profiles.

Figure 2.4 displays vertical profiles of observed radar reflectivity, Doppler velocity and lidar backscatter and the derived values of ice particle effective radius (r_e) and ice water content (IWC) obtained from a nadir pointing radar and lidar on board an aircraft overflying an extensive layer of cirrus during the recent ECAV campaign in Japan. The same retrieval algorithms (see Section 5.4) will be used with the lidar and radar embarked on the EarthCARE satellite to provide global profiles of these parameters. The IWC values will provide data to evaluate the performance of the models shown in Figure 2.2. Global observations of effective radius r_e can evaluate the current parameterisation of r_e as a function of temperature and suggest future NWP

parameterisation schemes in which r_e becomes a prognostic variable. Ice sedimentation velocities are crucial in NWP models in fixing ice cloud cover and lifetime; global observations of these velocities using Doppler radar will improve this crucial aspect.
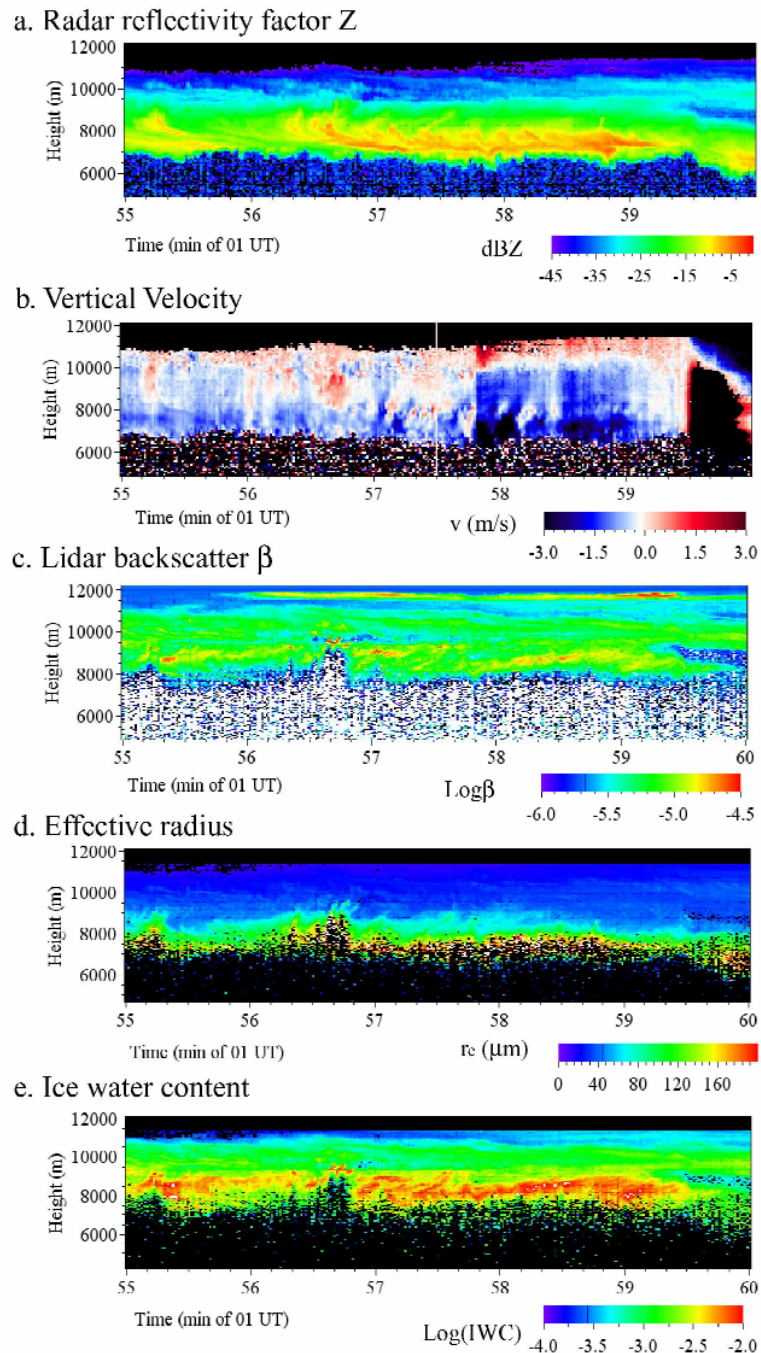

Figure 2.4: *Vertical profiles of observed radar reflectivity, Doppler velocity and lidar backscatter and derived values of ice particle effective radius (r_e) and ice water content (IWC) obtained from a nadir pointing radar and lidar on board an aircraft.*

2.6 Convection and Precipitation Processes

The majority of the Earth's rainfall results from convection – and especially so for the heavier precipitation such as displayed in Figure 2.5, which results in flash floods and loss of life. Yet convective precipitation is extraordinarily hard to represent within numerical models because it occurs on a scale which is much smaller than the grid box used in all models, and is essentially a statistical and noisy phenomenon. The current almost universal approach is based on a mass flux scheme whereby the stability of the vertical profile for each stack of grid boxes is examined at each time step, and if it is unstable then the scheme removes a fraction of the instability through a vertical mass flux. If this flux produces supersaturation and cloud, then precipitation may result. The fraction of the box involved and hence the updraft and fractional cloud cover is not explicitly derived. The performance of such schemes is often unsatisfactory, with such basic processes as the diurnal cycle of convection badly represented. New more physical schemes being developed favour a statistical approach in which, rather than a deterministic mass flux, the convection process itself is treated as a probability distribution function (PDF). Convection is indeed a statistical phenomenon and these PDF approaches capture this aspect, but different schemes lead to different PDF's of mass flux and vertical velocities, both in magnitude, cross-sectional area and vertical profiles, and sensitivities to initialisation schemes. Global observations of mass flux and vertical velocity profiles, which can be derived from the observations in Figure 2.5, are needed to evaluate these schemes. Apart from the occasional case study, there are currently no direct observations of velocities and fluxes.

The convection in Figure 2.5 overshoots the tropopause. Global observations are needed to quantify the amount of moisture introduced into the stratosphere by this process.

2.7 The Mission Objectves

The mission goal is to deliver observations of:

(a) Vertical profiles on a global scale of aerosol properties such as extinction coefficient (optical depth per unit height increment) and an estimate of the size and chemical composition of the aerosol particles differentiating between absorbing and non-absorbing aerosols.

(b) Vertical profiles on a global scale of cloud properties such as cloud cover, cloud overlap and the mass of liquid and ice water content condensed in the clouds, sub-grid-scale cloud inhomogeneity, and vertical velocities, cloud particle size and identification of the different types and shapes of ice particles present.

(c) Probability distribution functions (PDFs) of the mass flux and vertical velocities within stratiform and convective clouds and how such PDF's change with height, IWC and horizontal dimensions.
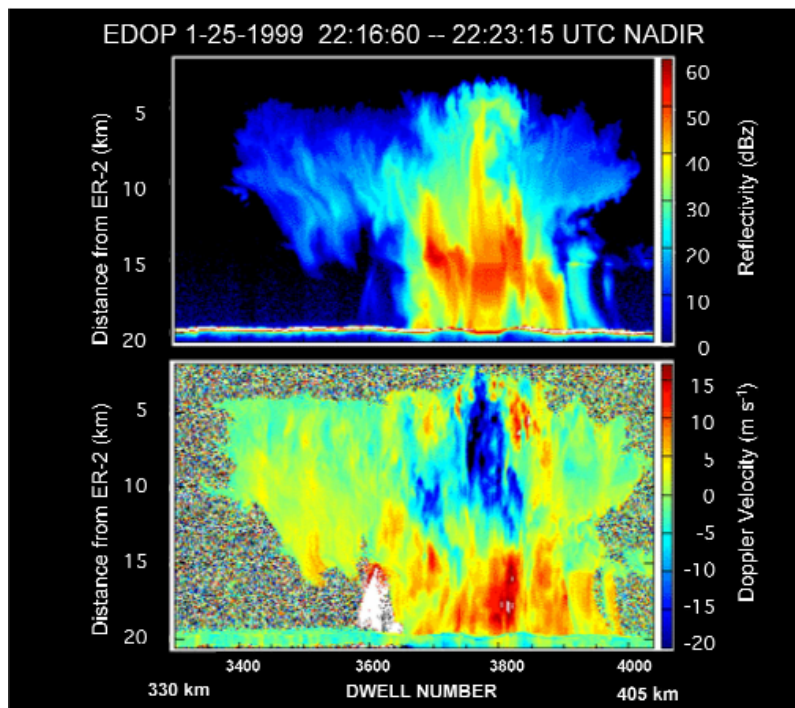
Figure 2.5: *Vertical cross section of radar reflectivity and vertical Doppler velocities observed from an X-band radar on the ER-2 aircraft overflying a severe tropical convective storm in Brazil (courtesy G. Heymsfield).*

Such observations will enable the performance of current NWP models and GCMs to be evaluated so that the various proposed schemes for parameterising aerosols, clouds and convective precipitation can be compared, any biases and errors within such schemes can be identified, and ultimately such schemes can be improved.

2.8   The Delta

The particularly new aspects of this mission are the embarkation on a single platform of a high spectral resolution lidar and a Doppler millimetre wave radar complemented by passive instruments to synergetically provide:

- Direct determination of the optical depth of the aerosol in the boundary layer.

- Independently derived vertical profiles of both the backscatter and the extinction coefficient of aerosols and clouds.

- Characterisation of the shapes and properties of aerosols and ice particles in clouds from the observed ratio of lidar extinction to backscatter and the lidar depolarisation ratio.

- Accurate profiles of ice water content and ice particle size from radar/lidar and imager synergy.

- Improved quantification of liquid water clouds including determination of drizzle fluxes and detection of supercooled water layers.

- Cloud inhomogeneities on the km scale.

- PDFs of vertical velocity including sub-grid scale motions.

- Observations of condensed water mass flux in convection including that penetrating the tropopause.

- Direct observations of ice particle sedimentation velocities in cirrus.

- Accurate drizzle and precipitation rates.

- Estimation of radiative flux gradients and hence heating rates at different vertical levels.

- The ability to verify the radiative self-consistency of the derived products.

3. Research Objectives

The EarthCARE mission has been specifically defined with the basic objective of improving the understanding of cloud-aerosol-radiation interactions so as to include them correctly and reliably in climate and numerical weather prediction models. Specifically, the scientific objectives are:

1. The observation of the vertical profiles of natural and anthropogenic aerosols on a global scale, their radiative properties and interaction with clouds.

2. The observation of the vertical distributions of atmospheric liquid water and ice on a global scale, their transport by clouds and their radiative impact.

3. The observation of cloud distribution ('cloud overlap'), cloud-precipitation interactions and the characteristics of vertical motions within clouds, and

4. The retrieval of profiles of atmospheric radiative heating and cooling through the combination of the retrieved aerosol and cloud properties.

The key parameters determining the radiative properties of clouds and aerosols are:

• The extinction and absorption properties of aerosols.

• Large scale cloud structure, including cloud fraction and overlap.

• Cloud condensate content, particle size, shape and small scale cloud structure.

Note that macroscopic and microscopic cloud parameters depend in part on physical and chemical properties of aerosols acting as cloud condensation and/or freezing nuclei.

EarthCARE will meet these objectives by measuring simultaneously the vertical structure and horizontal distribution of cloud and aerosol fields together with outgoing radiation over all climate zones. More specifically, EarthCARE will measure:

1. Properties of aerosol layers:

   (a) The occurrence of aerosol layers, their profile of extinction coefficient and boundary layer height, and

   (b) The presence of absorbing and non-absorbing aerosols from anthropogenic or natural sources.

2. Properties of cloud fields:

   (a) Cloud boundaries (top and base height) including multi-layer clouds.

   (b) Height resolved fractional cloud cover and cloud overlap.

   (c) The occurrence of ice and liquid and of super-cooled cloud layers.

   (d) Vertical profiles of ice water content and effective ice particle size and shape.

(e) Vertical profiles of liquid water content and effective droplet size.

(f) Small scale (1 km or less) fluctuations in these cloud properties.

3. Vertical velocities to characterise cloud convective motions and ice sedimentation.

4. Drizzle rain rates and estimates of heavier rainfall rates.

5. Narrow-band and broad-band reflected solar and emitted thermal radiances at the top of the atmosphere.

4. Observation Requirements and Measurement Principle

4.1 Introduction

The EarthCARE focus on aerosols and clouds addresses the two largest sources of uncertainty in current climate predictions. Aerosols provide the largest source of error in representing the direct *radiative forcing* of the climate system, while clouds provide the largest uncertainty in representing the *radiative feedbacks* than can either enhance or reduce the sensitivity of climate to that forcing (IPCC 2001). A component of the cloud feedback is also believed to arise from the *indirect effect* of aerosols on cloud radiative properties, so the two uncertainties are inextricably linked. The need for reliable information on the vertical structure of clouds and aerosol layers demands a unified observational approach that is uniquely provided by EarthCARE.

The basic structure and the variables represented in modern Numerical Weather Prediction (NWP) models are very similar to those in climate models, so EarthCARE data will also be utilised in this important, operational activity. The data can be used to initialise the model forecasts and also in the off-line evaluation of the representation of clouds. Aerosols are just beginning to be represented explicitly in NWP models and by the time EarthCARE is operational their inclusion in order to model atmospheric visibility and air quality is expected to be routine. Other expected applications for EarthCARE data include process studies in conjunction with in-situ airborne measurements and/or surface-based remote sensing, and the provision of vertically resolved cloud and aerosol information for adding value to the data from other satellite missions.

The specific observational requirements may be derived with reference to the cloud and aerosol parameters used in climate and NWP models and the horizontal and vertical resolutions with which these parameters are represented. The accuracy requirements are derived from estimates of the impact of changes in these geophysical parameters on the magnitudes not only of the local radiative heating, but also of the radiative fluxes at the top of the atmosphere. The latter provides a particularly useful constraint, as it may be quantified both by the accuracy with which broad-band radiances need to be modelled and by the accuracy with which they can be measured by the Broad Band Radiometer (BBR). In the following, we therefore firstly identify the required parameters and resolution and then proceed to estimate the required accuracy for each parameter.

4.2 Geophysical Parameters and Resolution

Climate and NWP models represent clouds in order to calculate the distribution of precipitation and the vertical profiles of solar and thermal radiative heating. Since the models cannot resolve individual clouds explicitly, the effects of such unresolved

processes on the grid-scale are *parameterised*, using statistical relationships which are derived from theory or observations. Similar considerations apply to aerosols.

For clouds, the variables that are represented explicitly in each grid box and at each vertical level are the fractional cloud cover, the liquid or ice water content and the size of water drops or ice crystals. The choice of ice water content terminal velocity has a profound effect on ice cloud lifetime. The parameterisations either assume or calculate the sub-grid-scale distribution or PDF of water substance and of cloud-scale vertical velocities and mass fluxes within convective clouds. Assumptions are then made about the vertical overlap between cloud layers in order to calculate the precipitation and radiative heating rates. Passive remote sensing provides some information on the geographical distribution of these variables as inferred from space, but very limited information on the vertical structure. The simulated radiative fluxes at the top of the atmosphere can usually be adjusted to agree with satellite observations, but different models achieve this result through radically different vertical distributions of cloud. Vertically resolved observations of clouds are urgently needed, to constrain the models and to test the ability of the parameterisations to represent the profiles of all of the cloudy variables mentioned above.

Similar considerations apply to aerosols, which are included in models both to represent their *direct effect* via radiative fluxes and surface forcing, and their *indirect effect* on cloud particle size, precipitation efficiency and radiative properties. The aerosol mass and size must be represented for several different aerosol types (e.g. sea salt, sulphate, dust, volcanic and carbonaceous aerosols from both natural and anthropogenic sources). Passive observations provide estimates of the aerosol optical thickness but, as with clouds, vertical information is required to distinguish different layers. A great deal of aerosol remains in the planetary boundary layer and so provides a tracer of the boundary layer depth. However, aerosols can also be lofted by convection above the scavenging effects of clouds and form persistent layers, the radiative effects of which depend strongly on height, which again emphasizes the need for observations of the vertical structure and estimates of convective motions. Estimates of aerosol absorption are needed because they affect cloud lifetime and would provide valuable additional information on the aerosol type. High resolution in the horizontal would enable the direct effects to be distinguished from those of clouds and the indirect effects on clouds to be investigated.

Typical values of the horizontal and vertical resolutions of current climate and NWP models are shown in Table 4.1 with values expected for the year 2010. Regional models with higher resolution are already used in both cases to provide local detail, or to resolve particular physical processes such as convection or severe storms. They will have resolutions close to 1 km by 2010. The use of such models provides two important links to EarthCARE. Firstly, by resolving explicitly more of the dynamical structures within which clouds form, the emphasis on model improvement moves to the representation of the small-scale physical processes within clouds and aerosol layers,

which are the primary focus of the mission. Secondly, the regional model resolutions are approaching the basic footprint size of the EarthCARE instruments, enabling direct model-to-satellite comparisons, which have hitherto been hindered by inadequate global model resolutions.

Parameter	Climate Models		NWP Models		Regional	
	Now	2010	Now	2010	Now	2010
Horizontal resolution (km)	250	100	50	25	10	2
Number of vertical levels	40	80	50	100	50	100
Vertical resolution (upper troposphere)	1.5 km	750 m	1 km	500 m	1 km	500 m
Vertical resolution (boundary layer)	200 m	100 m	100 m	50 m	100 m	50 m

Table 4.1: *Typical resolutions of climate, NWP and regional models.*

The values in Table 4.1 give the typical resolutions required for comparison of the EarthCARE products with models. However, the basic observational resolution needs to be as high as possible, not only to minimise non-linear effects on retrievals, but also so as to build up statistics on the sub-grid-scale distributions of cloud and aerosol quantities in 3 dimensions (e.g. the PDF of ice water content and cloud-scale vertical velocities).

Figure 4.1 summarises the scope of the EarthCARE mission.
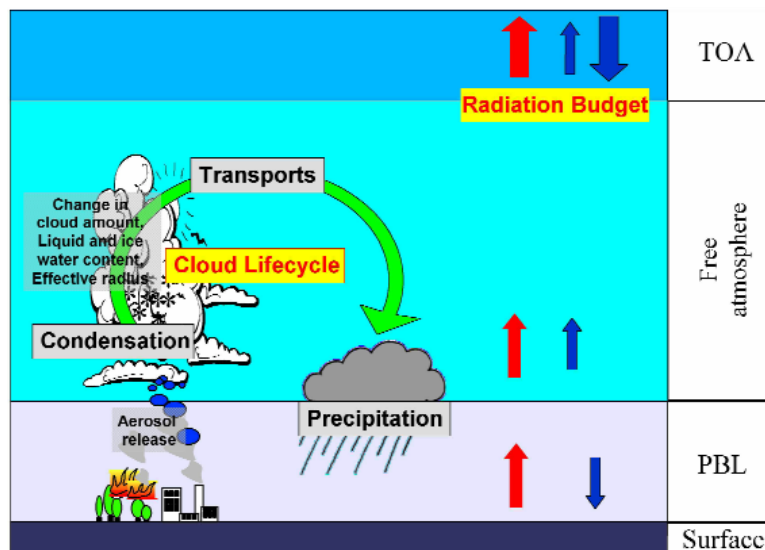
Figure 4.1: *The scope of the EarthCARE mission. The objective is to retrieve vertical profiles of cloud and aerosol, and characteristics of the radiative and microphysical properties so as to determine flux gradients within the atmosphere and fluxes at the Earth's surface, as well as to measure directly the fluxes at the top of the atmosphere and also to clarify the processes involved in aerosol/cloud and cloud/precipitation/ convection interactions.*

4.3 Accuracy Requirements

The accuracy requirements are based on typical values of the geophysical quantities provided by EarthCARE and on sensitivity calculations which provide estimates of 'radiatively significant' changes of about 10 Wm^{-2}, given the measurement capability of instantaneous radiances at the top of the atmosphere, which leads to the need to detect and measure clouds and aerosols with an extinction coefficient of 0.05 per km. Some of the requirements refer to a reference scale of 50 km, based on the information on the models in Table 4.1, although for many quantities the requirements also refer to the individual, pixel-level retrievals.

Table 4.2 summarises the requirements for clouds, based in part on the work of Slingo (1990) for liquid water clouds, Kristjánsson et al. (2000) for ice clouds, and calculations performed in earlier EarthCARE studies.

Property	Detectability Threshold	Accuracy
Ice cloud top/base and profile	N/A	500 m
Ice water content (IWC)	0.001 gm^{-3}	±30%
Ice crystal effective size	N/A	±30%
Water cloud top/base and profile	N/A	300 m
Liquid water content (LWC)	0.1 gm^{-3}	±15-20%
Water droplet effective radius	N/A	±1-2 μm
Fractional cloud cover	5%	5%
Ice cloud optical depth	0.05	15%
Vertical velocity within clouds	N/A	0.2 ms^{-1}

Table 4.2: *Accuracy requirements for cloud properties.*

The overlap of cloud layers in the vertical is an important parameter which is usually assumed in model parameterisations. The information on the cloud profiles in Table 4.2 will enable the overlap to be determined. The vertical velocity within clouds is presently also either assumed or modelled, as is the fall speed, or sedimentation rate, of ice crystals. Information on drizzle rates in boundary layer stratocumulus would be extremely valuable as this makes a significant contribution to the water budget of these clouds. Estimates of heavier rain rates would also be valuable.

The aerosol requirements have been calculated in earlier EarthCARE studies and may also be inferred from Cusack et al. (1998). The basic parameter required is the aerosol optical thickness profile. This needs to be converted into aerosol mass and size through additional information, for example on the aerosol extinction coefficient. Information on the aerosol type, even if only an indication of absorbing versus non-absorbing

aerosol, would be extremely valuable. A great deal of aerosol resides in the planetary boundary layer, so a well resolved measure of the aerosol height would also provide information on the depth of the boundary layer.

Property	Detectability Threshold	Accuracy
Optical thickness profile	0.05	10-15%
Top/base and profile	N/A	500 m

Table 4.3: *Accuracy requirements for aerosol properties.*

Other quantities that are required are listed in Table 4.4. These include the solar and thermal broad-band radiances at the top of the atmosphere. The accuracy requirement given is for an instantaneous measurement, consistent with an accuracy of 10 Wm^{-2} in the broad-band fluxes at the top of the atmosphere. Note that averaging in space and time provides fluxes with increased accuracy; for example, the values quoted for regional, monthly means are 5 Wm^{-2} from ERBE (Ramanathan et al. 1989) and 2 Wm^{-2} from CERES (Wielicki et al. 1996). The radiance requirement is based on the need to provide closure, by using the EarthCARE cloud and aerosol properties, together with additional information, to perform forward simulations of the observed radiances, as a final test of the retrieved properties. The accuracy requirements for the additional information needed to perform these calculations (surface temperatures and atmospheric temperatures and humidities) are not challenging and these quantities can be obtained from other sources, such as global NWP analyses.

Quantity	Detectability Threshold	Accuracy
TOA solar and thermal radiances	N/A	3 $Wm^{-2} sr^{-1}$
Surface and atmospheric temperatures	N/A	1.5 K
Atmospheric humidity	N/A	10%

Table 4.4: *Accuracy requirements for other quantities.*

4.4 Space/Time Sampling Requirements

The EarthCARE concept is motivated by the same scientific requirement underpinning the US Atmospheric Radiation Measurement (ARM) programme: the need for measurements of all the radiatively important constituents of the atmosphere. This will enable forward simulations to be made of the observed radiances at the top of the atmosphere and of the profiles of solar and thermal radiative heating rates in the atmosphere. Although there are fewer instruments, EarthCARE essentially provides a space-borne ARM site that visits every climate region on the planet. To do this, it is essential that all the instruments are flown together on one platform, because:

(a) This enables the fields of view of the different instruments to be co-located in space and time. Simultaneity between the various measurements is important because clouds vary rapidly in both space and time.

(b) This enables the height of the platform to be as low as possible, so as to optimise the performance of the active instruments.

A near-polar orbit is required to provide global coverage. Such orbits can be Sun-synchronous or can be designed to provide a slow drift in local time, to enable sampling through the diurnal cycle. While this option may appear to be attractive, in practice it can alias together the diurnal and seasonal variations so that the two are difficult to disentangle from the data. The preferred option is for a low-altitude, Sun-synchronous, near-polar orbit. The diurnal variations cannot be sampled from such an orbit, but they may be studied through comparisons with other satellites, particularly those in geostationary orbits.

4.5 Data Delivery

Real-time access to the Level 1 EarthCARE data is necessary if the data are to be assimilated into NWP models. Near-real-time access is needed for the evaluation of NWP models, to provide data for observational campaigns and for studies of current weather events. For climatological studies and the evaluation of climate models, delayed mode access (days to one month) is adequate.

4.6 Measurement Principles

The observational requirements discussed above indicate the need for measurements from a single satellite platform of the vertical structure of aerosols and clouds, plus complementary information on cloud-scale vertical velocities and precipitation, and of the corresponding broad-band and narrow-band radiances at the top of the atmosphere. The profile information can only be provided by active instruments, a lidar for aerosols and thin clouds and a high frequency (94 GHz) Doppler radar for clouds. These instruments can also provide the additional required information on discriminating absorbing from non-absorbing aerosols, on cloud-scale vertical velocities and precipitation (mainly drizzle) rates. A multi-spectral imager is required to provide additional geographical coverage of aerosol and cloud optical property retrievals, and a broad-band radiometer is required to measure radiances and to derive fluxes. These measurements need to be made for the whole globe and for a period long enough to ensure that all of the important climatic regimes are represented with the *necessary* statistical significance. This leads to the requirement for a single satellite mission with a lifetime of several years, in a Sun-synchronous polar orbit with as low an altitude as possible to optimise the performance of the two active instruments (lidar and cloud radar), which are supplemented by a multi-spectral imager providing cross-track observations and a broad-band radiometer for determining incoming and outgoing

radiation simultaneously. Additional information on atmospheric temperatures and humidity can be obtained from other sources.

The EarthCARE instrument combination must detect clouds and aerosols that have an extinction coefficient above 0.05 km^{-1} and are therefore considered to be 'radiatively significant', because they produce changes in radiative flux of at least 10W m^{-2}.

4.6.1   Lidar

Lidar is analogous to radar, but uses short pulses of light. The backscatter signal, β, at 355 nm has two components: a molecular (or 'Rayleigh') component from the air molecules which is proportional to air density, and a 'Mie' component from the aerosol or cloud particles. The return from cloud particles is approximately proportional to the their surface area and so $\beta \propto \Sigma N D^2$ in units of m^{-1} sr^{-1}, where N is the concentration of particles of size D, and the sum is over all values of D. Figure 4.2 (lower panel) from a ground based vertically pointing lidar shows the low values of β from aerosol in the boundary layer, the very large β but rapid extinction associated with liquid water clouds, and the moderate values of β and lower attenuation produced by ice clouds.
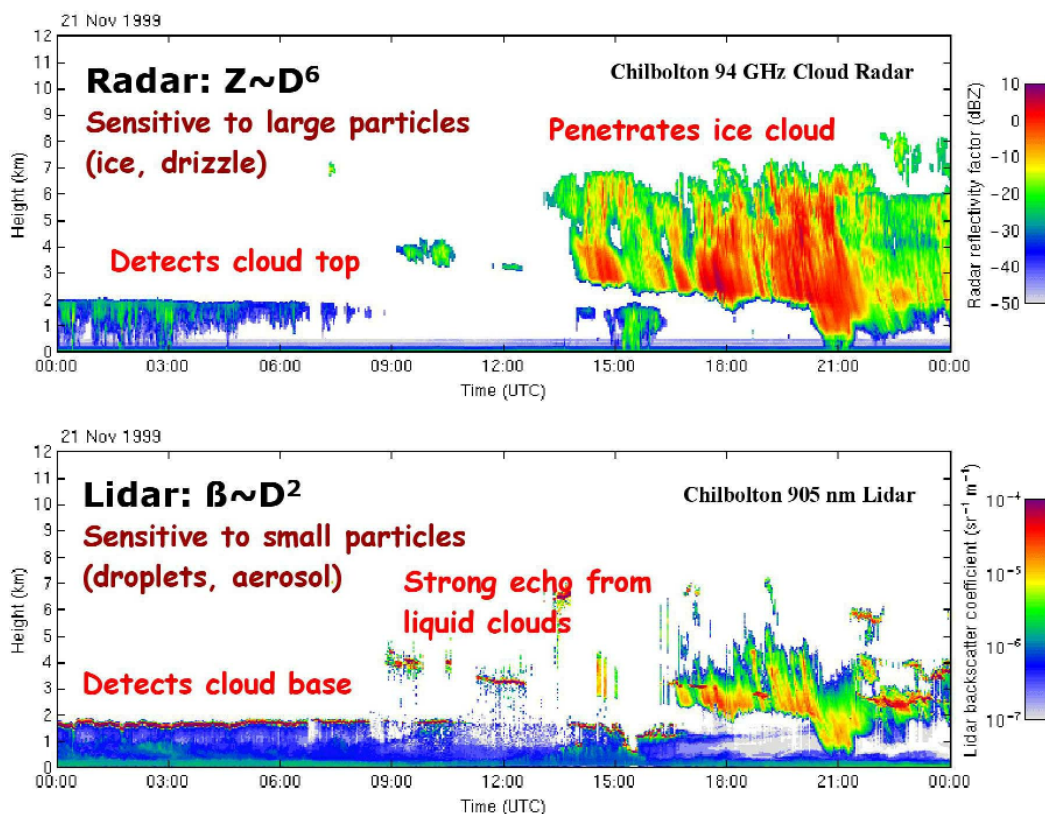

Figure 4.2: Radar/lidar from the ground to show aerosols below 2 km, liquid water clouds near 2 km producing drizzle, supercooled liquid clouds (3-6 km) and deeper ice clouds.

To detect an extinction 0.05 km^{-1} requires a sensitivity of $\beta = 8\times10^{-7}$(m sr)$^{-1}$ if we assume a ratio of the extinction to backscatter, α/β, of the lidar signal, S, of 60. Quantitative interpretation of the lidar signal, β, is difficult because of (i) attenuation in clouds, (ii) a variable and unknown value of S, and (iii) multiple scattering. For ice clouds, such as those in Figure 2.4, the radar signal can be used to correct for the lidar attenuation and derive the profile of the extinction coefficient to within 15%, independently of S. The ratio of the radar return ($Z \propto D^6$) to the corrected lidar backscatter then provides a measure of the mean ice particle size, and when combined with the radar return, the IWC and particle size can be estimated to an accuracy of 30% as shown in Figure 2.4 a,b.

In the case of aerosol no useful radar return is available and thus the lidar results alone must be relied upon. Conventional lidar designs can only measure the total aerosol and molecular return signals, but because the extinction-to-backscatter ratio of aerosol (S) is quite variable, it is difficult to estimate aerosol extinction. The EarthCARE lidar will separate the narrow band return from the slowly moving aerosol/cloud particles from the thermally Doppler broadened molecular signal. This 'High-Spectral Resolution' (HSR) technique uses any reduction in the molecular return to directly determine the extinction, α, of aerosols and thin clouds, which is then used to correct β in the Mie channel for attenuation, and find S. The HSR technique is similar in principle to the Raman lidar approach, in which the total Rayleigh and Mie return is separated from the wavelength shifted Raman scattered light from molecules. An example is shown in Figure 4.3 in which the independently derived backscatter and extinction profiles for
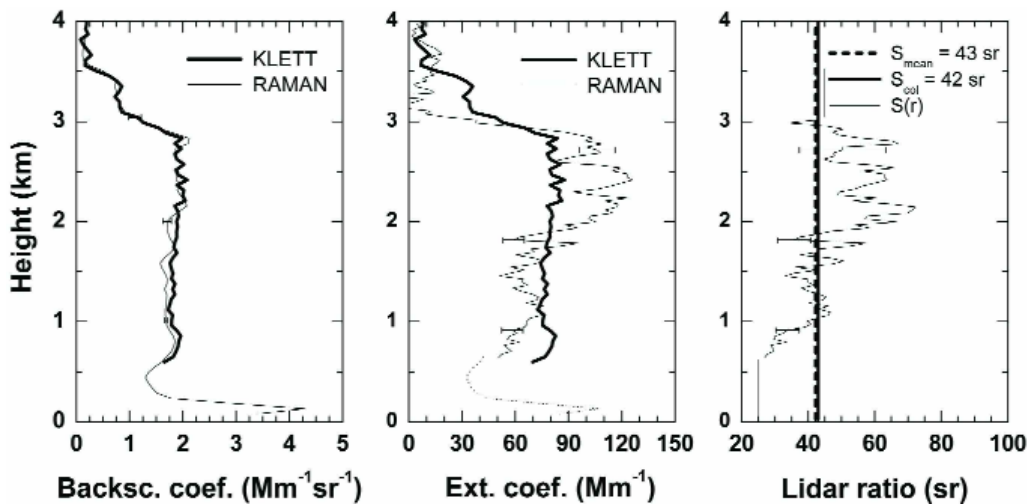
Figure 4.3: Raman lidar aerosol measurements made during the second Aerosol Characterisation Experiment in Portugal in summer 1997. Above the marine boundary layer (lidar ratio (S) 22.5sr) a pollution layer originating from Western and Central Europe was observed. Thick lines: results for the elastic signal alone (aerosol+molecular not separated) and an assumed value of S. Thin lines: more accurate results when both the molecular Raman and elastic signal are used. Similar results would be achieved using the HSR technique.

aerosols lead to values of S falling from about 60 at a height of 2 to 3 km to 22.5 below 1 km. In the case of a conventional elastic backscatter lidar with no clear air return under the aerosol layer, S cannot be derived and must be assumed. In general, the column average of S may vary by a factor of 3 to 5 depending on the (usually unknown) aerosol composition and size distribution. Even in the case where the assumed value of S is close to the true column average, large errors in the derived aerosol extinction profile may still result (compare the Klett and Raman results in the middle panel of Figure 4.3).

4.6.2 Cloud Profiling Radar (CPR)

The magnitude of the backscattered signal, or radar reflectivity, Z, is given by $\Sigma N\, D^6$, and is usually expressed in dBZ, that is in dB relative to the backscatter from a single mm raindrop in a cubic metre. The EarthCARE cloud radar will operate at 94 GHz frequency to maximise sensitivity and provide a narrow beamwidth even with a small antenna. Aerosol particles are very small and cannot be detected by radar. Liquid cloud droplets are typically 10 μm in size and are close to the threshold of detectability unless occasional drizzle drops are present (Fig. 4.2). Ice particles with generally larger size have a much larger value of Z (Figs. 4.2 and 2.4). Calculations using ice particle size spectra observed by aircraft show that a radar with a threshold of -36 dBZ will detect 98% of 'radiatively significant' ice clouds. The accuracy of the conversion of Z to IWC is limited to about 50-100% by the variability of the ice particle spectra; additional temperature information reduces this uncertainty to around 50%; more accurate size information can be obtained from the ratio of the radar signal to the attenuation corrected lidar signal as outlined in the previous section and shown in Figure 2.4. The smaller drops in liquid clouds makes them more difficult to detect. A year's climatology of radar observations indicates that only about 50% of stratocumulus clouds will be detected with a threshold of -36 dBZ; derivation of liquid water content from Z is difficult because Z is dominated by occasional larger sized drizzle drops; however, when drizzle is present the Z is related to the drizzle rainfall rate.

The EarthCARE CPR will be the first space-borne radar with a Doppler capability. There are two scientific requirements: firstly to characterise convective motions, an accuracy of 1 ms^{-1} with a horizontal resolution of 1 km is necessary; and secondly to estimate the sedimentation of ice particles in cirrus. An accuracy of 0.2 ms^{-1} is desirable at the expense of 10 km horizontal resolution. Once the vertical velocity is known, then the product of the velocity and the IWC derived from either the radar alone or in combination with the lidar will yield an estimate of the mass flux. Doppler velocities are derived by measuring the change in phase of the return from two successive transmitted pulses separated by pulse interval time (inverse of pulse repetition frequency (PRF)): the maximum unambiguous velocity (folding velocity) corresponds to a phase change of ±180 degrees. Doppler measurement from a moving space platform is a challenge because the Doppler spectrum width of the target increases due to the large Doppler velocity signals arising from the finite antenna

beamwidth and large platform ground speed of about 7 kms^{-1}. This effect leads to a rapid decorrelation of the target signals and results in only a small correlation between the two consecutive pulses unless PRF is high enough. The highest PRF is defined by the requirement that the observation window is greater than the height of the atmosphere. The radar PRF value must be chosen to be as high as possible depending on the satellite altitude in orbit. Although the folding velocity is ±5.6 ms^{-1} for a PRF of 7 kHz, ambiguities can be resolved by considering velocity continuity. The off-nadir platform attitude error will cause a Doppler velocity error. Correction to this error could be made by consulting satellite navigation data or by referring Doppler signals from the surface echo.

An example of the Doppler velocity profiles measured by high flying aircraft above a cirrus cloud deck is shown in Figure 2.4 and above a *vigorous* tropical convective storm overshooting the tropopause in Figure 2.5. Gettelman et al. (2002) suggest that at any one time such penetrative convection occurs over 0.5% of the tropics. To achieve Doppler measurements from space, a 2.5 m antenna is essential, otherwise the phase information between successive transmitted pulses is lost. A 94 GHz radar can provide information on rain-rates of up to 10 mm hr^{-1} (l'Ecuyer and Stephens 2003) before attenuation becomes too severe. Low rainfall rates associated with drizzling stratocumulus (e.g. Fig. 4.2, 0 h-6 h) are important in determining their evolution and persistence. In stratocumulus, the cloud and drizzle contributions to Z can be separated using the Doppler information, and thus the rain rate over the range 0.001-1 mm hr^{-1} can be deduced.

4.6.3 Multi-Spectral Imager (MSI)

MSI retrievals use the spectral information of radiances or apparent reflectance, which depend on the optical characteristics of atmospheric suspended particles, aerosol and cloud particles. For optically thin layers the radiances are mostly proportional to the sums of the differential cross sections and attenuated radiances reflected by surfaces. For the ocean surface, since the albedo is low, the reflected component is exactly estimated by the assumed particle parameters, whereas for the land surface the surface albedo has to be estimated in order to account for the generally non-negligible surface reflection. It is therefore difficult to retrieve the aerosol parameters over high reflectance surfaces such as desert and snow. Over dark vegetation surfaces, clear-day statistics of radiances and correlation between radiances at a specified wavelength and a longer near infrared wavelength, such as 1.6 μm and 2.2 μm, is used to retrieve the surface albedo. After removing the surface reflection component at each wavelength, the ratio of aerosol path radiances gives a good index of Ångström exponent or effective particle radius of aerosols. After obtaining the size index, reflectance is used to retrieve the optical thickness (Higurashi and Nakajima 1999).

On the other hand, the apparent reflectance for an optically thick cloud layer is mostly a function of optical thickness in a non-absorbing channel and a function of cloud

particle size in the near-infrared channel. Therefore, use of a pair of wavelengths in the visible and near-infrared retrieves optical thickness and cloud particle size (e.g. Kawamoto et al. 2001). Cloud top temperature is also estimated by infrared channel accounting emissivity of cloud that depends of optical thickness and effective radius. The radiances of three thermal infrared channels are used to determine cirrus optical thickness, effective radius and temperature in daytime and nighttime (Katagiri and Nakajima 2004).

4.6.4 Broadband Radiometer (BBR)

The objective is to derive accurate instantaneous broadband TOA fluxes (reflected shortwave, SW, and emitted longwave, LW) corresponding as much as possible to the small areas for which the radar, lidar, and MSI provide data. The BBR measures radiances emergent from TOA fields of view of order 10 km, using principles and techniques that have demonstrated their effectiveness in the Nimbus/ERB, ERBE, ScaRaB, and CERES missions (e.g. Wielicki et al. 1996, Duvel et al. 2001). As in CERES, ScaRaB, and (in practice) ERBE, broadband LW radiance is obtained by subtraction of broadband SW radiance from total channel radiance. Spectral correction for residual spectral filtering of the BBR optics and sensors is performed following procedures developed and applied in ERBE, ScaRaB, and CERES, involving knowledge of the instrument spectral properties together with scene identification to estimate scene spectral signature. Accurate *instantaneous* radiance-to-flux conversion is ensured by the 3-view configuration of the BBR, building on experience with CERES, POLDER, and MISR data to use the additional nearly simultaneous off-nadir views of the nadir pixels.

5. Mission Performance Estimation

The observational requirements for EarthCARE place performance demands on each individual instrument as well as the instrument package as a whole. In order to ensure that the proposed instrument package satisfies the mission goals, analyses of radar and lidar observations have been conducted along with extensive simulation activities. This chapter begins with a brief overview of the expected performance of each instrument. A discussion on the use of the active instruments alone to retrieve particle size and optical extinction profiles and the accuracy of the resulting predicted flux profiles is then presented. Finally, sample results from simulations that illustrate the performance of the mission as a whole (active together with the passive instruments) are presented. This is complemented by a summary of the achieved geophysical performances.

Details about the technical concept can be found in the technical dossier.

5.1 Active Instruments

Lidar

The need to detect clouds and aerosols that have an extinction coefficient above 0.05 km^{-1} (see sub-Section 4.6.1) leads to the requirement that the lidar must detect values of Mie backscatter greater than 8×10^{-7} (m sr)$^{-1}$ for a vertical resolution of 300 m and an along-track integration of 10 km. Also, in order to directly estimate the optical thickness of cirrus clouds and aerosol to within 0.05, relative changes between the Rayleigh (molecular) return signal between two different altitude ranges must be able to be determined within 10%.

Detailed simulations have shown that the small instrument footprint size does not eliminate multiple-scatter effects. However, the magnitude of the effects are of the order of those commonly encountered with conventional ground-based lidars, and can be accounted for using established methodologies.

Radar

The radar detectability threshold should be -36 dBZ at the top of the atmosphere for a 10 km along-track integration (see sub-Section 4.6.2) or -31 dBZ for 1 km integration with 500 m vertical resolution. This threshold will enable the radar to detect over 98 and 92%, respectively, of radiatively significant ice clouds. The Doppler performance with a 2.5 m antenna for the tropical (6400 Hz) and high latitude (7200 Hz) PRF is shown in Figure 5.1 At high latitudes, velocities can be measured to better than 0.2 m s^{-1} for 10 km horizontal integration provided Z is > -18 dBZ, which, from the airborne analysis, includes 96% of the ice mass flux in cirrus. Convective motions in the tropics can be estimated to 1 m s^{-1} with 1 km horizontal resolution for Z > -17 dBZ, which should detect 95% or the tropical cirrus ice mass. The EarthCARE radar will oversample the return signal every 100 m vertically. This will help better determine

cloud boundaries and separate the surface contribution from the cloud contribution for low clouds.
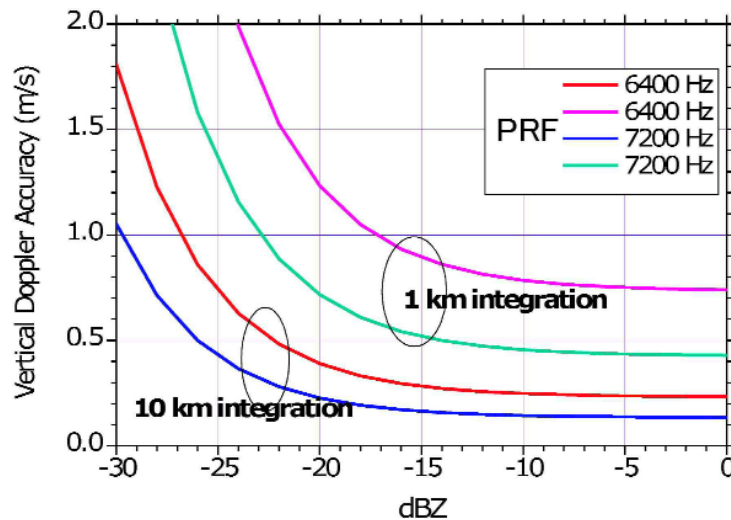

Figure 5.1: *Doppler performance with a 2.5 m antenna and a tropical (6400 Hz) and high-latitude (7200 Hz) PRF for 1 and 10 km along-track integration.*

5.2 Passive Instruments

Multi-Spectral Imager (MSI)

The MSI will have channels at 659 nm, 865 nm, 1.61 μm, 2.2 μm, 8.8 μm, 10.8 μm and 12.0 μm. The MSI will measure radiances in a 150 km swath consisting of 500 m square pixels. The MSI will be used to infer cloud and aerosol properties as well as to provide information on the cloud variability on the 500 m scale. For the first 4 bands single pixel reflectances will be measured with a SNR ratio of 200 for a solar zenith angle of 15˚. The radiometric stability will be better than 1% over one year and the absolute accuracy will be better than 10%.

Broad-Band Radiometer (BBR)

The BBR will measure top of atmosphere (TOA) reflected solar and emitted terrestrial radiation. The instrument will have three views (nadir and 55˚ forward and backward relative to the line of flight) with a pixel size of 10 km. The radiometric resolution and absolute accuracy will be better than 1.5 W m^{-2} sr^{-1} in the short-wave and long-wave channels.

5.3 Co-Registration and Sampling

In order for the EarthCARE instruments to be used together, the instrument footprints and sampling intervals have been formulated in a co-ordinated fashion. The EarthCARE instruments have the following sampling characteristics:

- Lidar: an along-track linear row of footprints less than 30 m in diameter separated every 70-100 m.

- Radar: a footprint on the order of 750 m with virtually continuous data accumulation. Signals are reported up to a frequency of approximately 1 km intervals (the exact interval will be slaved to the lidar sampling).

- MSI: 500 m square footprint with a 150 km swath perpendicular to the flight path.

- BBR: To improve co-registration with the other instruments, oversampling will be used to provide 10 km square footprints every 1 km for each of the three views.

The relative relationship between the footprints of the lidar, radar and MSI is sketched in Figure 5.2. Here the 'worst-case' separations between the footprint centres are shown. In particular, the maximum offset between the lidar and radar boresight and the centre of the MSI nadir pixel is within 350 m RMS (goal of 200 m RMS). Simulations based on data acquired by aircraft and ground-based lidars and radar have shown that the pointing requirements and the proposed sampling strategy ensure that full synergistic use can be made of the multi-instrument data.
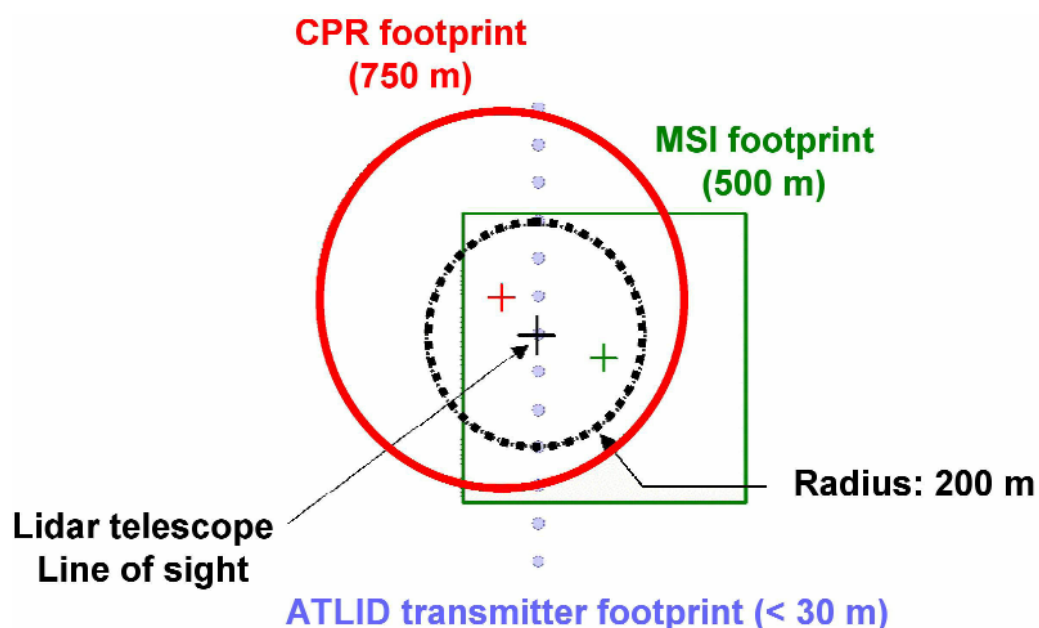
CPR footprint (750 m)

MSI footprint (500 m)

Radius: 200 m

Lidar telescope Line of sight

ATLID transmitter footprint (< 30 m)

Figure 5.2: EarthCARE instrument footprints and 'worst-case' misalignments.

5.4 Radar-Lidar Synergy for Identifying Supercooled Clouds

Supercooled layer clouds contain only small droplets and so can be identified by their very high lidar backscatter leading to rapid attenuation but which is unaccompanied by any increase in the radar reflectivity (see Fig. 4.2). Such supercooled clouds are important because the small amount of liquid water has a very large radiative effect compared to the same mass of ice cloud, but they are poorly, if at all, represented in

current models. Analysis of the 10.5 hours of lidar observations in Figure 5.3 taken during the LITE experiment aboard the Space Shuttle from 40° to 60° N shows the frequency of cloud occurrence as a function of cloud temperature and the fraction of these clouds which contain a supercooled layer; comparison with one year's ground based observations at Chilbolton, UK reveals that the fraction of cloud containing supercooled layers was almost identical to those observed from space, although from the ground the presence of low clouds frequently obscured the higher clouds. Virtually no supercooled clouds colder than -40°C were observed, but at -10°C about 20% of clouds contained supercooled layers.
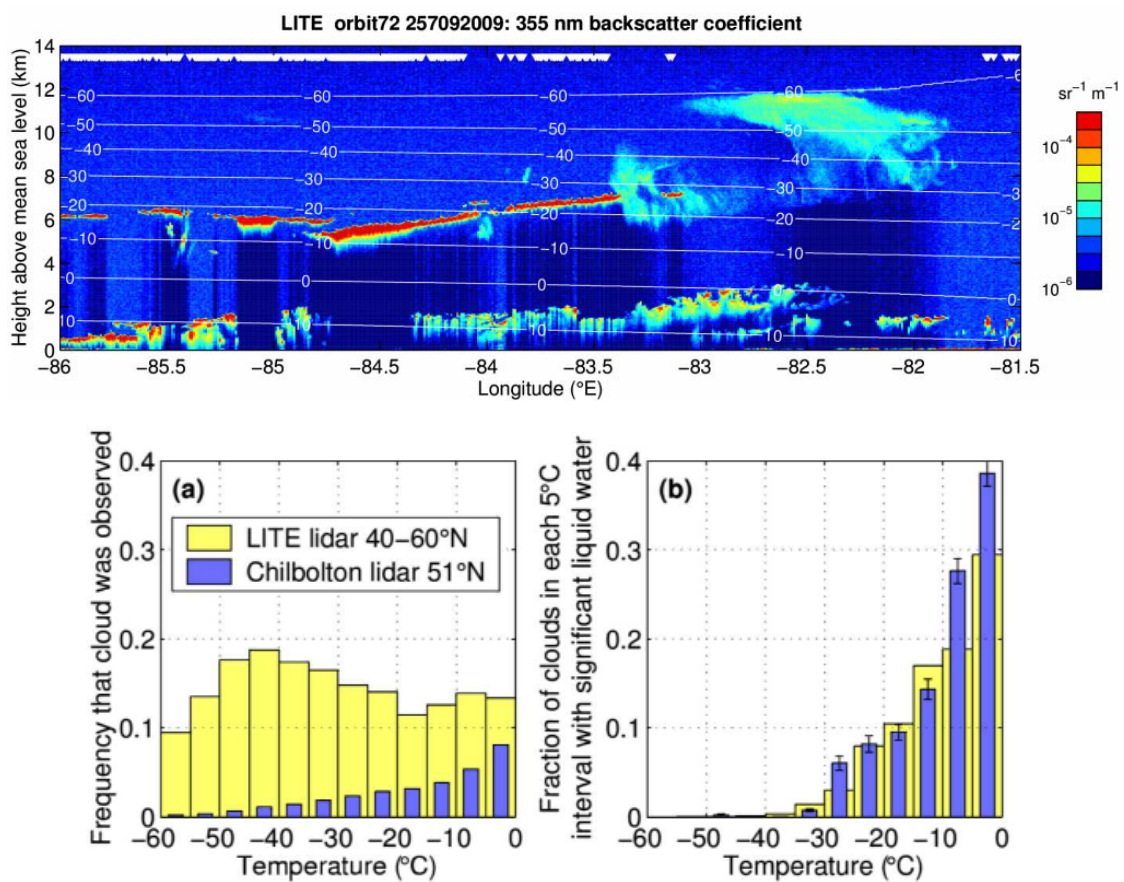

Figure 5.3: *Comparison of lidar observations from LITE (above) between 40° N and 60° N and from Chilbolton at 51° N: (a) fraction of pixels above 2 km observed to be clouds; (b) fraction of clouds in each 5 K temperature interval containing a supercooled layer.*

5.5 Lidar/Radar Inversion Algorithm Blind Tests

To gauge the performance of the active instruments in retrieving accurate profiles of short- and longwave radiative fluxes within ice clouds, a series of blind tests has been carried out. In these tests (Hogan et al. 2004) vertical profiles of radar and (attenuated) lidar returns in ice clouds together with profiles of shortwave and longwave radiative

fluxes were computed. These calculations were based on data from in-situ aircraft observations of the ice particle size spectra using an assumed ice density as a function of size and an assumed value of S. The profiles were then adjusted for the radar and lidar sensitivities specified in Section 5.1 and the correct instrumental noise statistics introduced with 100 m oversampling of the radar signal and the effects of lidar multiple scattering included. A typical lidar profile with and without the instrumental response and multiple scattering is displayed in Figure 5.4.
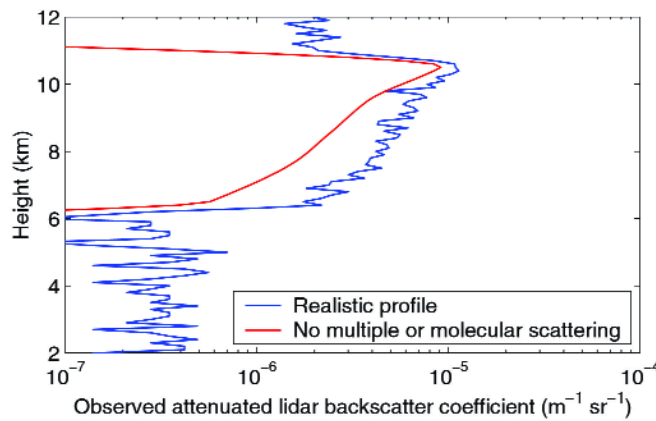

Figure 5.4: The attenuated lidar backscatter coefficient profile computed from the aircraft profiles and given to the authors of the blind test.

The computed profiles of instrument returns, but not the value of S, were then given to the authors of the two retrieval techniques (Donovan et al. 2001, and Tinel 2002). These techniques avoid the usual problem with the instabilities that arise with gate-by-gate correction schemes by introducing a constraint from the radar to maintain a stable solution in the last few gates, either at the bottom of the cloud or just before the lidar signal is extinguished, whichever is sooner. For the Donovan routine, the constraint is that the 'radar-lidar effective radius', R'_{eff}, proportional to $(Z/\alpha)^{0.25}$, is approximately constant in the last few gates, whereas for Tinel, the ice particle concentration N_o^* parameter proportional to $\alpha^{1.71}/Z^{0.71}$, is approximately constant in this region. The first guess is found by picking a moderate value for optical depth, τ, and using it to derive the extinction profile, α, from the attenuated β profile. By combining this with the radar reflectivity measurements, N_o^* or R'_{eff} are calculated. τ is then adjusted iteratively to minimise the gradient in N_o^* or R'_{eff} in the last few gates.

Figure 5.5 demonstrates that the extinction profile of the cloud is accurately retrieved independently of the actual value of S; even if S is variable with height, the retrieved values are stable and the total optical depth is accurate. Figure 5.6 shows that the retrieved upwelling longwave flux is also accurately retrieved to within the specified 5-10 W m^{-2} provided the effects of multiple scattering are included. This impressive accuracy arises because the longwave fluxes are fixed by the extinction profile of the cloud. The accuracy of the shortwave fluxes is not quite so good in most cases because

the albedo also depends somewhat on the asymmetry factor and single scattering albedo, which vary with effective radius. The different values of effective radius in Figure 5.7 demonstrate the error introduced when the retrieval makes different assumptions about the abundance of small crystals in the distribution; the extinction is completely independent of these assumptions. Further tests were carried out with denser clouds leading to extinction of the lidar signal so that a combined lidar/radar retrieval was not possible in the lower part of the cloud. The retrieved optical depth in the upper part of the cloud controls the outgoing longwave radiation which can still be accurately estimated. The shortwave fluxes are more error prone because the total optical depth of the cloud is important, not just the first 1 to 2 optical depths at cloud top as for longwave. Two approaches are being explored for this situation. Firstly, the albedo can be independently estimated from the MSI instrument. Secondly, a specific Z-extinction relationship is derived from the upper part of the cloud where full retrievals are possible, and then this relationship, appropriately scaled, is used to derive the extinction profile from the observed Z in the lower part of the cloud. The blind tests show this second approach can be remarkably successful.
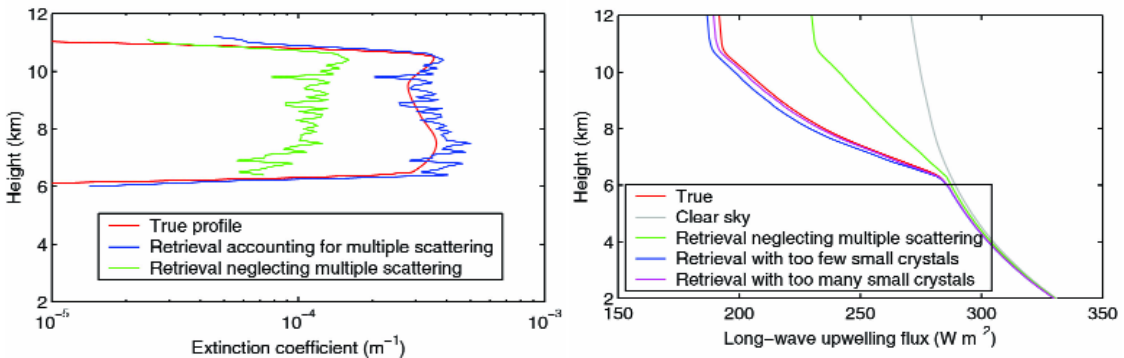

Figure 5.5: The retrieved extinction profile produced by the blind test algorithm with and without multiple scattering.
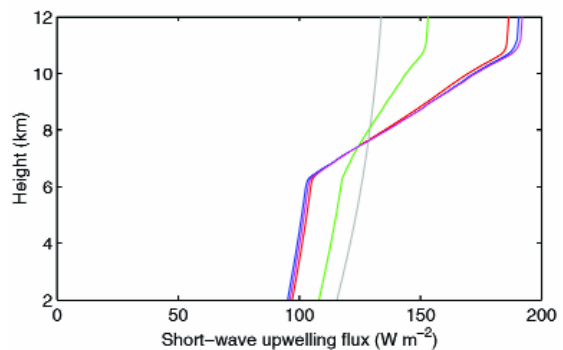
Figure 5.6: The retrieved longwave and shortwave fluxes from the blind test algorithms compared with the original true values.
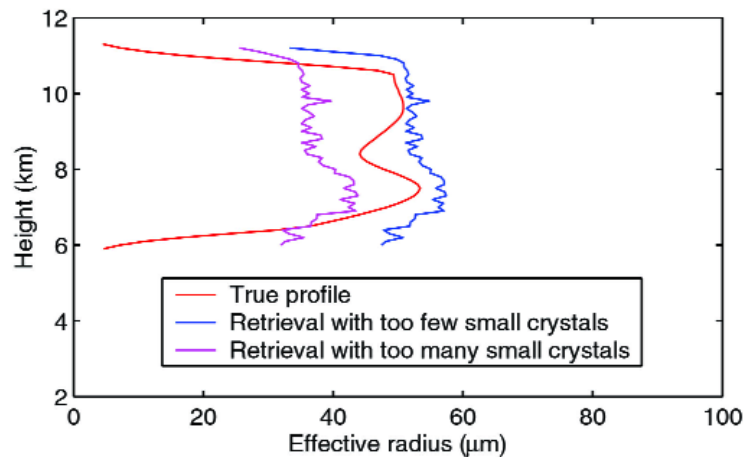
Figure 5.7: *Dependence of the retrieved effective radius on the assumed particle size spectrum.*

It should be stressed that very accurate extinction profiles can be derived from the radar/lidar algorithm, but the derived values of R_{eff} and IWC are less certain. This is a very fortunate result because it is the extinction profile that dominates the radiative fluxes. The GCMs have a more difficult task, because they have IWC as a prognostic variable and, using a prescribed r_e, then have the problem (which the instruments have circumvented) of computing the extinction profile.

5.6 Simulation Results

In addition to the algorithm intercomparison studies, detailed simulation studies have been conducted. A hypothetical cloud scene corresponding to a 10 km track (the size of a BBR pixel) is shown in Figure 5.8 and the top two panels of Figure 5.9. The situation depicts an ice cloud of varying optical thickness (2 in the physically thin section and 4 in the thicker section) that partially overlaps a stratus deck of optical thickness 4 with an effective particle size of 10 µm. Covering the lower 2 km of the scene is a boundary layer sulphate aerosol field with a visible (500 nm) optical depth of 0.1. The predicted co-polar Mie and Rayleigh and cross-polar signals along with the radar reflectivity are shown in the remaining panels. The simulation results shown were carried out under daylight conditions taking expected instrument noise into account. The lidar simulations were based on a detailed Monte-Carlo multiple-scatter model, which also predicts the polarisation state and spectral state of the return signal. The effect of non-ideal spectral separation between the molecular and aerosol/cloud signals have also been taken into account. The radar simulation results take into account such factors as the pulse width and the effects of speckle and thermal noise. The lidar simulations are shown at a 100 m horizontal and vertical resolution, while the radar has a horizontal resolution of 0.5 km and the return is oversampled every 100 m in the vertical.
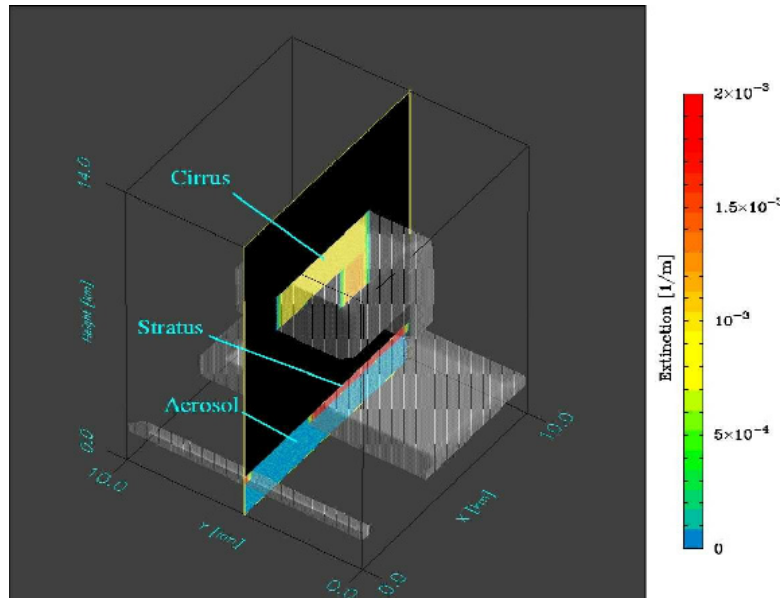
Figure 5.8: *Extinction field corresponding to an ice cloud of varying thickness over a partial stratocumulus deck.*
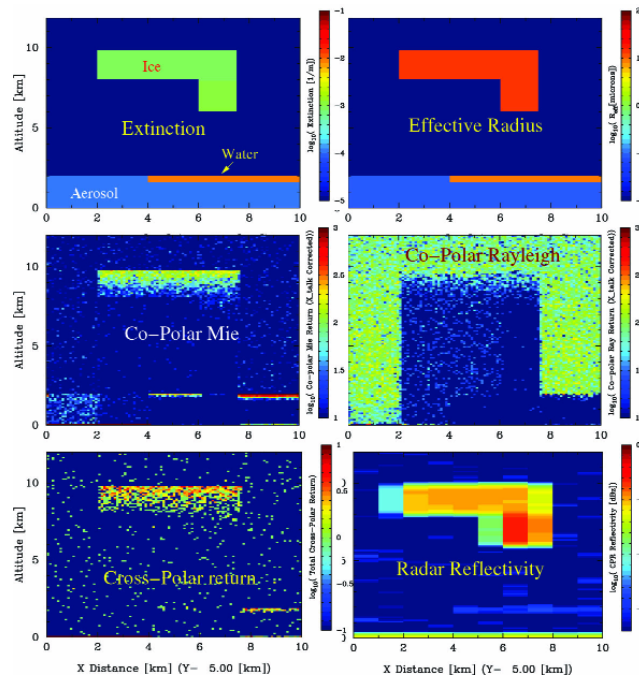
Figure 5.9: *Simulated idealized scene containing ice cloud, water cloud and aerosol. Shown are the extinction at 500 nm (top-left) and the effective radius field of the scatterers (top-right). The other panels show the expected lidar and radar signals taking into account instrument and background noise and non-ideal instrument behaviour. Here the lidar data is shown with a resolution of 100×100 m while the radar data has a resolution of 500 m in the horizontal.*

The 'views from the top' for four MSI channels are shown in Figure 5.10. Here two VIS/near-IR and two thermal-IR simulation results for nadir viewing and a solar zenith angle of 30˚ over ocean are shown. The results were generated using 3D Monte-Carlo short- and longwave models using the same data as for the lidar and radar simulations. The Sun is at an azimuthal angle of 50˚ (i.e. out of the lower left corner of Figure 5.10) giving rise to the shadows present in the 0.86 and 1.3 μm channel images.
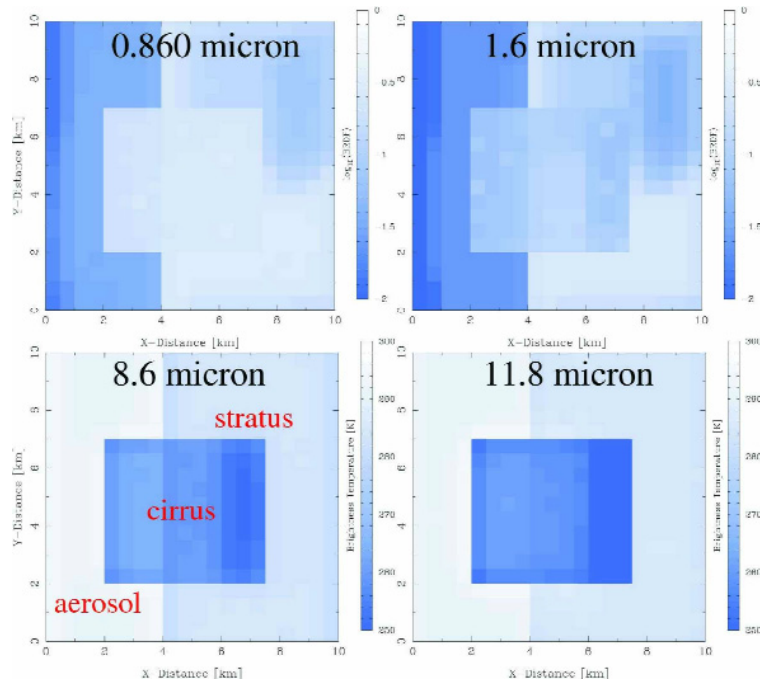

Figure 5.10: *The 'view from the top' as seen by four of the MSI channels for the same scene as depicted in Figure 5.9 for a solar zenith angle of 30˚ and azimuth of 50˚. Note the sensitivity of the 8.6 an 11.8 μm channel results to the total optical depth of the overlapped cirrus and stratus clouds. The pixel size here is 500×500 m, which corresponds to the resolution of the MSI.*

Though idealized, Figures 5.9 and 5.10 succinctly illustrate the capabilities (and limitation) of the lidar, radar and MSI and demonstrate how the different instruments complement each other. The proposed lidar designs are capable of detecting all radiatively significant targets (i.e. optical depth greater than 0.01 at the 10 km horizontal scale). However, the lidar signal is subject to large attenuation. Thus in Figure 5.9 the lidar detects the presence of the aerosol when no higher cloud is present. Under the thin parts of the cirrus clouds, the presence of aerosol is on the edge of detectability (with 1 x 0.3 km averaging) and the underlying water cloud is easily detected. Under the thicker part of the cirrus, the lidar signal is completely extinguished and not even a surface return will be registered. The radar suffers practically no attenuation from the ice cloud and has no difficulty detecting the entire extent of the ice cloud. However, the reflectivity levels of the stratus deck are just at the detectability threshold of the radar (on the 0.5 km scale). From above, the VIS/NIR channels are

subject to 3D effects with respect to the cloudy pixels. However, the unshadowed aerosol pixels can be used to determine aerosol optical depth and Ångström coefficient. The MSI channels also demonstrate the sensitivity of the TOA radiances and brightness temperatures to the cloud composition and optical depth. In particular, areas of overlapped, non-overlapped, and thick and thin areas of cirrus can be distinguished in Figure 5.10. The thermal IR channels are particularly useful for determining the cloud properties here, as they are not as affected by 3D radiative transfer effects.

Aerosol Profiling

The EarthCARE lidar will also allow boundary layer aerosol optical depth to be determined with minimal assumptions. With a HSR capability, for aerosol extending to the ground, it is possible to determine the extinction by comparing the backscatter signals from above and below the aerosol layer. However, the Rayleigh channel can still be used to determine aerosol optical depth, independent of assumptions as to the nature of the aerosol, or the nature of the underlying surface. This is a unique advantage over non-HSR type lidars in space. An example retrieval of the extinction and backscatter profiles for a simulated 2 km thick boundary layer aerosol profile is shown in Figure 5.11. This is the same aerosol field as used in Figures 5.8 and 5.9 without the cloud
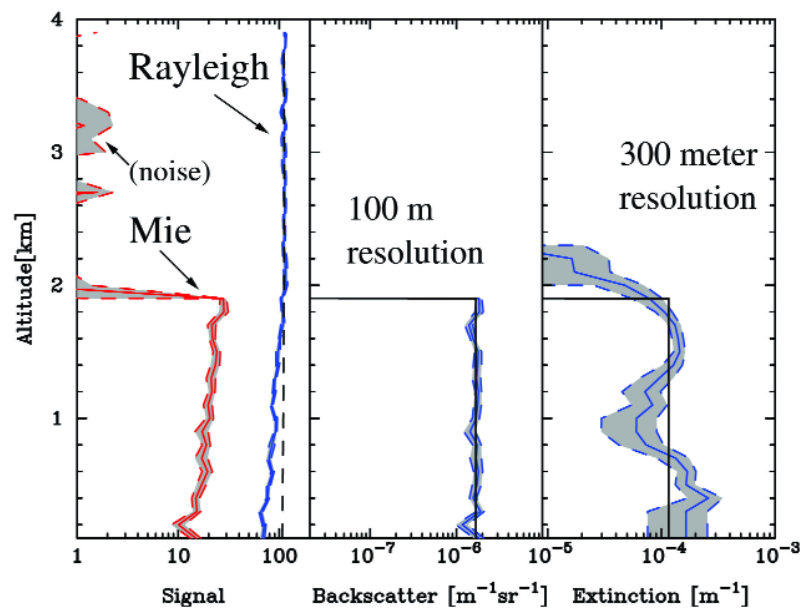
Figure 5.11: Simulated molecular and Mie signals (corrected for cross-talk) for a simulated boundary layer sulphate aerosol profile with a total optical depth of 0.1 at 500 nm (0.2 at 355 nm). The other panels show the retrieved extinction and backscatter coefficients. The process of deriving the extinction involves taking a vertical derivative of the signal and thus the retrieved extinction is noisier and has a lower resolution than the corresponding backscatter profile retrieval. The simulated data shown here represent a 10 km average under full daylight background conditions (no clouds are present over the aerosol layer).

cover. In this situation, a conventional lidar sounding can only determine the backscatter profile; to estimate the extinction, a backscatter-to-extinction ratio (which can range over an order of magnitude) must be assumed. With the HSR lidar the extinction-to-backscatter ratio at 355 nm can be determined, which can then be used to aid in the determination of the aerosol type. For example, S in the range of 60-70 sr typically indicates the presence of anthropogenic particles, while values of S less than 30 are typically associated with maritime aerosols (Mattis et al. 2004). In this example, the retrieved optical thickness of the BL aerosol layer is retrieved to within 10%.

5.7 End-to-End Results

End-to-end simulations have been carried out for a number of idealized cases (such as that depicted in Figure 5.8) as well as scenes derived from cloud resolving models. In these end-to-end trials the combined lidar/radar and nadir pixel MSI data has been used to construct optimal estimates of the profiles of the nadir cloud optical and microphysical properties. Then the information in the nadir profiles was propagated outwards to fill-out the nadir BBR 10 × 10 km pixel using the non-nadir longwave MSI pixel radiances. In essence, for a given non-nadir pixel, the closest matching (in terms of measured LW radiances) nadir pixel was determined, then the derived cloud and aerosol properties corresponding to that pixel were assigned to the non-nadir pixel in question.

After the reconstructed three-dimensional cloud property fields were created, they were fed back into the 3D longwave and shortwave Monte-Carlo radiation codes in order to calculate the TOA fluxes and the BBR radiances. Finally, the reconstructed TOA fluxes and broadband radiances were compared with the 'true' values. For example, for the scene shown in Figures 5.8 to 5.10, for a solar zenith angle of 40˚ the shortwave albedo from the reconstructed scene is 0.249, while the true value is 0.244 (the incoming shortwave radiation is 1044 W m^{-2}). The true longwave flux for this scene is 238.6 W m^{-2}, while the reconstructed scene has a value of 237.3 W m^{-2}. For this idealized case the combined short- and longwave TOA flux error is well within the 10 Wm^{-2} instantaneous accuracy goal. It should be pointed out that while the scene used in this demonstration is idealized, it a complex non-plane parallel scene and not amenable to conventional MSI retrieval approaches based on plane-parallel theory.

Other simulations have been conducted using data from cloud resolving models with explicit microphysics. An example of the model 'true' 355 nm optical depth field corresponding to a mid-level cirrus cloud compared with the reconstructed field is shown in Figure 5.12. For this scene, the TOA shortwave albedo can be reconstructed within a 5 to 6% error for a range of solar zenith angles between 20˚ and 50˚.

The end-to-end simulations that have been carried out as part of the Phase-A studies for EarthCARE will also be applied in a similar manner to the operational data. That is, the comparison between the observed broad-band BRDF's and the retrieved BRDF will serve

as an important test of the accuracy of the overall retrievals. If the retrieved and observed BRDFs match, then a high level of confidence can be assigned to the inferred TOA fluxes.
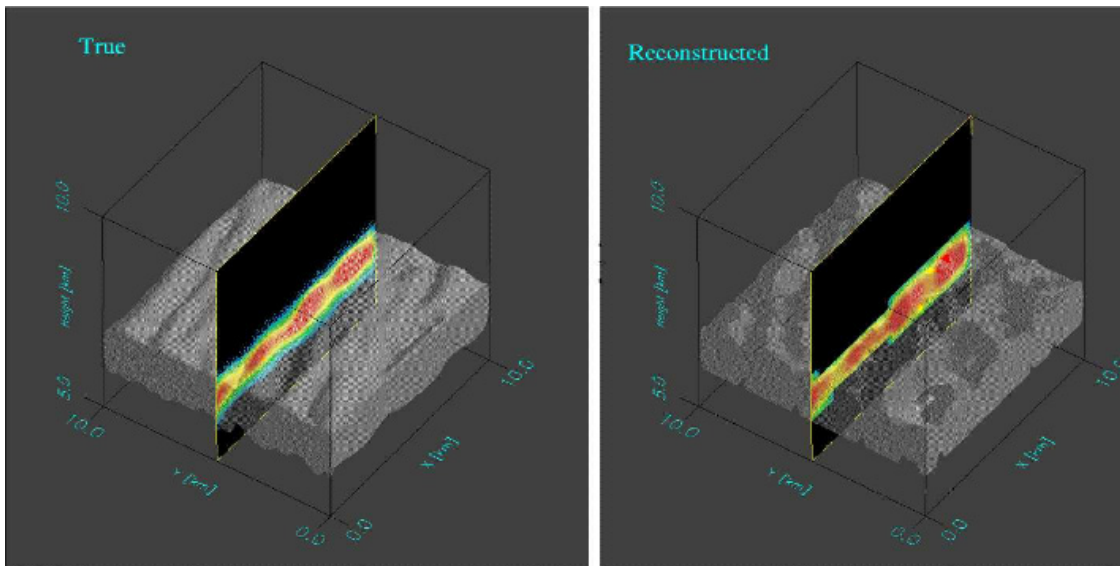
Figure 5.12: *Left: True 355 nm cloud optical thickness for a mid-level cirrus generated by a cloud resolving model with explicit microphysics. Right: Reconstructed optical thickness.*

The simulations that have been conducted show that the combined EarthCARE sensors will enable the retrieval of a radiatively complete picture of a wide range of cloud and aerosol scenes at the 10 km scale. An important component of the envisaged EarthCARE retrieval procedures will be the ability to check the self-consistency of the retrieval products.

5.8   Performance Summary

High Spectral Resolution (HSR) Lidar

The HSR lidar will be able to detect Mie scatter as low as 8×10^{-7} (m sr)$^{-1}$ with a vertical resolution of 100 m with an error of 50%. Rayleigh backscattering will be detected with a vertical resolution of 300 m with an error of 15% error at 9 km height and within 20% at a height of 0.5 km. A 10 km horizontal integration applies in all cases. For a cirrus cloud with a backscatter coefficient of 2.6×10^{-5} (m sr)$^{-1}$, if the true depolarisation ratio is 10% the cross-polar sensitivity leads to an estimate of between 5 and 15% for a horizontal resolution of 100 m.

This level of performance will allow several important items to be derived from the EarthCARE lidar:

1. By averaging the Rayleigh return for 1.2 km above and below a cirrus cloud 9-10 km in height with an optical thickness of 0.05, the total optical thickness may be determined with an error of 80%, and for an optical thickness of 1 with only a 15% error. Within cirrus clouds, profile measurements of the extinction coefficient may be made. The accuracy will depend on the resolution and optical depth into the cloud. For example, for a vertical resolution of 0.5 km and horizontal resolution of 1 km, the extinction coefficient may be determined within 60-80%.

   The Rayleigh channel extinction measurements will be supplemented by those from the Mie channel and radar backscatter described below and in Section 5.5. This will provide a useful consistency check on the measurements.

2. For a 1 km deep boundary layer with an optical thickness of 0.2 at 355 nm, the optical depth may be derived to within 10-15% on the 10 km horizontal scale (see Fig. 5.10). The corresponding lidar ratio (S) can be determined to within about the same accuracy and will enable the discrimination between aerosol types.

3. The cross polar channel will be able to distinguish between ice clouds (depolarisation typically higher than 20%; Reichardt et al. 2002) and water clouds (where depolarisation due to multiple-scatter effects will typically be below 5%). In areas of elevated aerosol loading, the depolarisation ratio will be useful in identifying the presence of non-spherical aerosols such as desert dust, which can have lidar depolarisation ratios in the range 10-25% (Ansmann et al. 2003).

Doppler Cloud Radar

The radar detectability threshold will be -36 dBZ at the top of the atmosphere for a 10 km along-track integration (see Section 4.6.2) or -31dBZ for 1 km integration with 500 m vertical resolution. From analysis of aircraft tropical ice particle images, this threshold will enable the radar to detect over 98% and 92%, respectively, of radiatively significant ice clouds. For mid-latitude stratocumulus, the figures are 52% and 44%, respectively, and about half of the detected clouds will be drizzling. At high latitudes, the Doppler velocities (Fig. 5.1) can be measured to better than 0.2 ms^{-1} for 10 km horizontal integration provided Z is above -18 dBZ, which means that the sedimentation velocity of 96% of the ice mass flux in cirrus can be estimated and accurate rain-rates from drizzling stratocumulus can be determined. Convective motions in the tropics can be estimated to 1 ms^{-1} with 1 km horizontal resolution for Z above -17 dBZ, which should detect 95% of the tropical cirrus ice mass and provide invaluable information about the ice mass flux of convection penetrating into the stratosphere.

Combined Lidar and Radar

(a) In ice clouds, using the algorithms in Section 5.4 to correct for attenuation and multiple scattering for cloud optical depths up to 3 or 4, the profile of extinction can be estimated to ±15%, independent of assumptions about particle size distribution, habit, mean extinction–to-backscatter ratio or even instrument calibration errors. Radiative transfer calculations show that these extinction errors lead to errors in longwave flux profiles of only 2 Wm^{-2}. Uncertainty in the mass-size (i.e. density) relationship of the ice particles leads to error of 30% in the ice water content, particle size and extinction-to backscatter (i.e. particle habit) profiles and 6% in the shortwave fluxes compared to the clear sky values. MSI data should reduce this albedo error. For deeper clouds that the lidar does not penetrate, the longwave fluxes above the region not penetrated are still equally accurate, and shortwave fluxes are more accurate than those from radar alone retrievals.

(b) Identification of super-cooled clouds by low radar backscatter and high lidar signal.

Multispectral Imager (MSI)

The MSI provides context for the nadir profile measurements, and the nadir pixels be used together with the lidar and radar to improve the lidar/radar retrievals. In addition, by itself the MSI can provide a large number of 'standard products', e.g. cloud optical depth and column average effective radius. As an example, for a 'plane parallel' water cloud with an optical thickness of 5 and an effective particle radius of 10 microns, the optical thickness may be estimated to within 5% and the column effective radius to within ±2 microns on the 1 km scale.

In water clouds, the lidar backscatter profile, usually only available in the top portions of the cloud, may nevertheless (by assuming quasi-adiabatic cloud behaviour) be useful in conjunction with visible MSI radiances, and in determining stratocumulus microphysical properties. Accurate lidar cloud tops will also improve MSI retrievals that use the thermal IR radiances. In thick water clouds, the integrated backscatter in the Mie channel will provide an accurate independent means to calibrate the Mie channel of the lidar (O'Connor et al. 2004).

Visible optical depth estimates derived from the MSI visible channels can also be used in conjunction with the radar reflectivity in order to estimate stratus cloud properties (Austin et al. 2001). For ice clouds, IR radiance retrievals may be greatly improved by using cloud boundary information provided by the lidar and radar (Cooper et al. 2003).

Broad Band Radiometer

By itself, the three-view instrument will enable total TOA fluxes to be estimated within 8.7 Wm^{-2} for plane parallel situations. Used in conjunction with the MSI and the lidar

and radar soundings, the instantaneous TOA flux measurements are expected to be well within this range even for complex non-plane-parallel situations at the 10 km scale.

EarthCARE analyses (BBR-MSI synergy) will benefit from CERES and ScaRaB experience of combining narrow- and broadband data to improve radiance-to-flux conversion and estimates of in-atmosphere and surface as well as TOA longwave and shortwave fluxes. Improving on ISCCP experience, forward radiative transfer calculations using retrieved cloud and aerosol profiles (lidar and radar) will provide narrow-band radiances to be checked by MSI data, and tri-directional broadband radiances to be checked by BBR data.

EarthCARE as a Whole (Lidar+Radar+MSI+BBR)

Identifying the presence of most clouds with 1km horizontal resolution and 500 m in the horizontal means that, for a 30 km size model grid box, cloud fraction can be estimated to within about 5%, and the degree of overlap in a vertical stack of grid boxes can be determined. In addition, the sub-grid scale PDFs of water content and convective motions can be derived.

End-to-end simulations, examples of which were shown in Section 5.6, have demonstrated that EarthCARE will be able to provide flux profiles consistent with a TOA error of less than 10 Wm^{-2}, as required in Chapter 4, even in complex and non-homogeneous cloud fields. This will be achieved by inverting the EarthCARE measurements in a coherent fashion. TOA radiances may then be calculated using the inversion results and then checked against the observed values. The possibility to conduct such self-consistency checks is an important aspect of this mission. This capability will ensure that EarthCARE will deliver on its promise of providing high-quality data to the broader scientific community.

6. Data Processing Requirements

Many of the algorithms for retrieving the required cloud parameters such as profiles of cloud extinction, ice water content, particle size and radiative flux profiles already exist and will be further developed by the time EarthCARE is launched. The techniques that will be employed in the analysis of EarthCARE data range from well established methodologies (such as the retrieval of cloud optical depth and effective radius from MSI radiances; Nakajima and King 1990) to recently developed synergetic algorithms involving multiple instruments (i.e. Austin and Stephens 2001, Cooper et al. 2003, Donovan 2003, Okamoto et al. 2003). Some of the more recent developments in the applied use of multisensor techniques have been described in Chapter 5. This chapter outlines how the global data set to be obtained from the EarthCARE satellite could be used to evaluate the representation of clouds in operational models and the work being carried out to set up a system for assimilating the cloud data into operational models.

6.1 Ground Based Evaluation of Clouds in Operational Models

Analysis of ground based vertically pointing radar and lidar profiles has been compared with the representation of clouds in the operational mode grid box above the ground-based station. An example of one day's cloud radar and lidar profiles with 30 second temporal and 60 m vertical resolution is provided in Figure 4.2. The operational model holds values of cloud fraction and IWC each hour with a vertical resolution of between 200 and 500 m, so cloud fraction can be derived for each model grid box from over 100 observations of cloud/no-cloud and grid box IWC from the mean reflectivity. Figures 6.1a, c and d display mean observed profiles of cloud fraction and IWC for the period May 1999 – May 2000 together with the corresponding values from the UK Met Office and ECMWF models. Figure 6.1a shows that the mean cloud fraction is in fairly good agreement, but the ECMWF model is overestimating the occurrence of cloud below 2 km by a factor of two. Figure 6.1c reveals that for mid-level clouds there is an underestimation of the mean fraction of cloud when present by both models. The horizontal blue lines in Figure 6.1d are the uncertainty in the retrieval of IWC from the observed Z. The errors shown here are larger than those using the EarthCARE algorithms. They show that although the mean value of IWC in the model for mid-level clouds is rather less than observed, the values are within the observed error bars. This agreement is much more reassuring than the large spread in IWC from AMIP shown in Figure 2.2. More recent comparisons of cloud fraction for April–October 2003 are shown in Figure 6.1b and confirm that the modification to the clouds scheme in ECMWF has successfully removed the excess low level cloud apparent in Figure 6.1a.

The improved sensitivity of the radar in 2003, -31 dBZ at 10 km, means that it is no longer necessary to remove the high altitude, low IWC cloud from the model which the radar could not detect (Figure 6.1a). This new data does, however, confirm that both models have too much cloud above 8 km by as much as a factor of two. EarthCARE will extend such comparisons to a global scale.
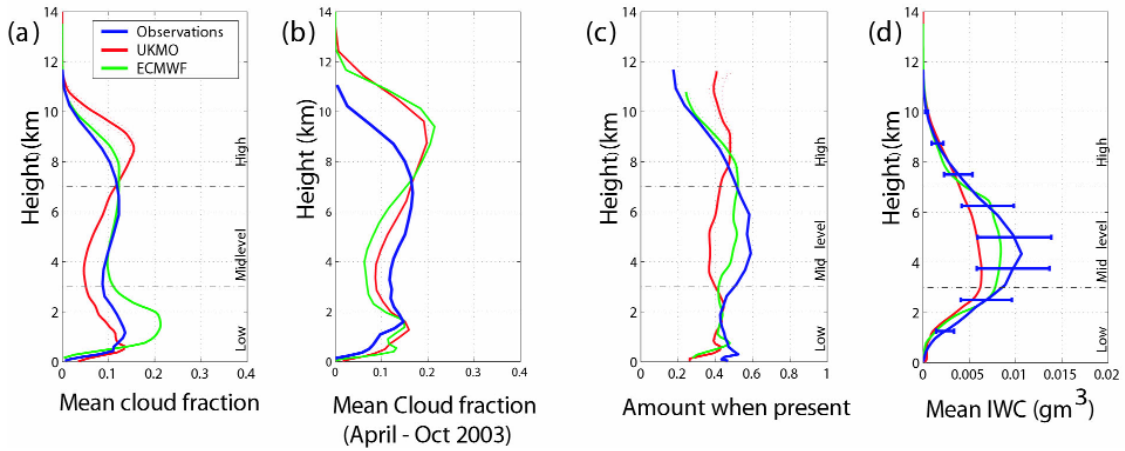
Figure: 6.1: Mean profiles, as observed by cloud radar and lidar at Chilbolton and output from the UK Met Office and ECMWF forecast models of (a) cloud fraction for May 1999 to May 2000, and (b) for April-October 2003, and for the 1999-2000 period: (c) mean cloud fraction when cloud is present, and (d) mean ice water content.

6.2 Assimilation of Cloud Data

Despite the importance of clouds and precipitation in the atmosphere, there is no explicit analysis of clouds and precipitation operational in global data assimilation systems in current operational models. The first steps in setting up such an analysis are being taken at ECMWF, where incremental four-dimensional variational assimilation (4D-Var) is used as an operational data assimilation system. Variational assimilation techniques assume linear processes, so clouds and precipitation present a problem because they are very non-linear and not at all smoothly varying. As a consequence of the changes in clouds (cloud cover, liquid/ice water content), top of the atmosphere radiation fluxes are also modified. An adjoint technique applied to the radiation parameterisation scheme can be used to investigate how large changes in cloud variables (or other meteorological variables) will lead to the certain change of TOA radiation fluxes in the model. The adjoint provides a gradient of an objective function J, (for example, top of the atmosphere short- or longwave flux) with respect to an input variable (such as cloud fraction), given the gradient of J with respect to output variable (radiation flux). These gradients provide information on the meteorological variables to which the parameterisation schemes are most sensitive and they can give some indications related to the importance and efficiency of using particular types of observations in the model. When the technique is used in the global model, the spatial and temporal patterns of the various sensitivities can be investigated. Figure 6.2 shows the results of these experiments for the effect of cloud fraction on shortwave and longwave fluxes at the top of the atmosphere during the winter. The shortwave fluxes are most influenced by the warmer water clouds, particularly in the Southern Hemisphere because of the increased insolation during the southern summer. The longwave pattern is rather different. Here the greatest sensitivity occurs when changes

to the amount of cold high cloud occur, with a subsidiary maximum at the freezing level. At low altitudes, the clouds are similar in temperature to the surface, so their presence has little effect on the upwelling longwave radiation at the top of the atmosphere.

Figure 6.2: Sensitivity of radiative flux to cloud fraction (dF/dc) for (a) shortwave and (b) longwave radiative flux for Northern Hemisphere winter – zonal mean values show radiative flux levels reaching 10 to 15 W m^{-2} in the tropics and in the summer hemisphere.

Preparation of the ECMWF system for the assimilation of the cloud- and radiation-related observations is being carried out. By the time EarthCARE is launched, the ECMWF will be able to assimilate cloud observations operationally.

7. User Community Readiness

The prime users of EarthCARE products will be climate and weather forecasting communities. Given the large uncertainty in the treatment of the aerosol-clouds-radiation-precipitation processes in climate simulations and in weather forecasts, the EarthCARE mission is expected to produce an unprecedented improvement in model reliability.

EarthCARE will provide a unique set of observations that will be used for an improved understanding of energy and water fluxes in the atmosphere and of the mutual interactions of clouds, aerosols and radiation. This in turn will have direct application in improving numerical models for operational weather forecasting and for climate prediction. The data will be an invaluable source of information for model validation, the improvement of physical parameterisations, and as input for data assimilation systems and their future development.

7.1 Global Model Validation and Improvement

The shortcomings in the treatment of cloud and aerosol processes in climate and numerical weather prediction (NWP) models arise primarily from the lack of observations for validation of cloud and aerosol parameterisation schemes. EarthCARE is expected to yield new insights into the divergence of radiative energy, interactions between clouds, aerosols, and radiation, vertical distribution of liquid water and ice water and their transport by clouds, cloud field overlap and horizontal structure as well as cloud-precipitation interactions. Comparison of numerical model results with data provided by EarthCARE will be used to identify model biases in the representation of clouds, radiation and aerosols, and to understand the origin of these biases. Consequent improvements will enable atmospheric models (a) to depict not only an accurate current climate, but also its variability and sensitivity to changing forcings, so important for climate change studies, and (b) to provide more accurate and reliable weather forecasts including those for severe weather with associated high societal impacts.

7.2 Improving Physical Parameterisations

The large uncertainties in the description of the cloud and radiation processes in NWP models are known to have a significant influence on medium range forecasts. The EarthCARE data will be used for process studies over a large range of different climatic regimes. The better understanding of the basic physics in these regimes will enable parameterisation schemes to properly represent this global diversity. Developments aimed at subjecting climate models to similar NWP-type validations are well advanced (e.g. the Transpose-AMIP/CAPT projects) and will ensure that EarthCARE data will impact directly on climate model evolution.

The climate modelling community is making large efforts to improve the aerosol and cloud physical processes, such as super parameterisation modelling (e. g. Randall et al., 2003), and to increasing a model resolution to take in finer general circulation and vertical motion with a large-scale computer system, such as the Earth Simulator run by JAMSTEC. The important issue in these improvements is better simulation of vertical structure of aerosol, water vapour, convective motion and clouds. EarthCARE with its high horizontal and especially vertical resolution will provide very useful data sets to tune and validate the climate models and to reduce climate prediction errors.

Current satellite instruments constrain the total incoming and outgoing radiation at the top of atmosphere, but cannot provide sufficiently accurate determinations of cloud profiles and consequent energy heating profiles. There are no such global datasets, which would simultaneously provide the vertical profiles of clouds and aerosol characteristics together with vertical temperature and humidity profiles and the TOA radiances. However, the vertical profiles are important in controlling the radiative transfer processes in the atmosphere, and so affect the heating profiles, which then influence the dynamics. The EarthCARE instrument complement will have the unique ability to provide global information on the profiles of clouds and aerosols in a radiatively consistent manner.

A representation of aerosols is also important for both climate prediction and global monitoring purposes. Changes in aerosols can directly modify the solar radiation reaching the ground, and also affect microphysical, biochemical and photochemical processes in the atmosphere and clouds. In addition, increases in aerosols resulting from human activities can have indirect radiative effects due to increasing the cloud albedo by decreasing the droplet size, modulating the precipitation processes, and changing the cloud lifetime. This indirect aerosol forcing could be very important and new measurements are therefore essential.

The radiative transfer in atmospheric models requires assumptions about cloud overlap and particle sizes. The overlap assumptions affect both the radiative transfer and the precipitation efficiency of the clouds. Any observations to evaluate whether this representation is correct are of crucial importance as there are scarcely any observations of this kind. Quantitative information on the ice water path would help to reduce significantly the level of uncertainty related to the modelled ice phase. Information on the depth and water content of the widespread tropical ice clouds is also missing and would be very useful for improving parameterisation schemes.

Increasingly, the development of new schemes for clouds and convection is utilizing information on the statistical properties of in-cloud vertical velocities. EarthCARE will provide unique global access to such information previously available only from field experiments for individual cloud systems.

Following extended site measurements like ARM and aerosol or cloud type targeted regional campaigns (ASTEX, APEX, INDOEX, BALTEX, ACE, ABC and similar) in recent years, a growing interest and potential for application to improve parameterisation in climate models is apparent in a substantial number of publications in this field. The surface observation network already provides good coverage of the globe with comprehensive instrumentations including radiometers, automatic lidar, aerosol counters etc. There are several facilities operating cloud profiling radars (GAW, ARM, AERONET, SKYNET etc). All would provide unique validation capabilities for the EarthCARE mission.

7.3   Data Assimilation

Pressure, temperature, water vapour and wind information from conventional and satellite observations have been operationally assimilated at NWP centres for more than two decades. Clouds are obvious measures of atmospheric humidity variations due primarily to vertical motions, yet there is still no explicit assimilation of cloud information and generation of cloud analyses in operational global forecasting systems. With the recent improvements in the representation of clouds (such as the development of prognostic cloud schemes) and dynamically consistent data analysis systems (such as four-dimensional variational assimilation), it is becoming possible to assimilate observations in cloudy situations in an effective manner. Currently, the cloud contribution to satellite radiances is removed from the assimilation systems. This creates an inconsistency between the non-cloudy regions of the atmosphere that have been modified by observations, and cloudy areas that are not changed. Research studies on the use of real-time satellite data in cloudy and rainy areas are already in progress in some operational centres with promising results. These studies will lead to a proper methodology for the inclusion of cloud profile information provided by the EarthCARE instruments in data assimilation systems. For this purpose, the data would be most valuable if available in near-real-time, even if just on a 'best effort' basis.

While objective forecasting skill has improved at a rate of at least one day per decade, the detailed prediction of weather parameters such as precipitation and cloud cover is rather less impressive and still subject to inaccurate descriptions of the moist processes and their specification in the initial conditions for the forecast. The assimilation of cloud observations will lead to an improved initial state for the dynamical and thermodynamical variables linked to the generation and dissipation of the clouds. Moreover, atmospheric analyses created with EarthCARE data will be the most reliable space-time description of global cloud properties and hence ideal for validating climate models. Furthermore, the systematic comparison of EarthCARE products with shortrange model forecasts will lead to improved specification of forecast error of cloud variables, necessary for the improvement of the data assimilation process. The unique synergy between active and passive instruments onboard EarthCARE will enable one to identify the conditions for which information derived from passive instruments alone can match the vertically resolved information gathered from the

active-passive combination on EarthCARE. Such an exercise is useful for, model validation as well as data assimilation.

7.4 Conclusions

The climate modelling and numerical weather prediction user communities are well prepared: (a) to handle the observations, and (b) to exploit the unique data set provided by EarthCARE. By 2010, limited-area forecast models will have horizontal resolutions that will be able to use EarthCARE data at full resolution (Table 4.1). There are already new developments in embedding cloud-resolving models into a GCM, which will - in the long term - converge into global cloud-resolving assimilation and forecasting systems.

8. Global Context

8.1 Other Planned Missions

At present, most of the cloud and aerosol parameters are derived from passive instruments. Crude assumptions are made to derive these properties. Almost no direct information on the vertical structure of clouds and aerosol fields is available.

A first step in the direction of measuring cloud and aerosol with active techniques was (after LITE in 1994) the launch of ICESAT in January 2003. While the driver for this mission is observation of ice sheet surface elevations with high accuracy, the lidar can also provide observations of atmospheric properties. No similar mission is planned for the time of the EarthCARE mission.

In recent years, the space agencies of the US (NASA), Japan (JAXA, formerly NASDA) and Europe (ESA) have developed plans for satellites carrying active remote sensing instruments like radar and lidar for cloud observations. Japanese, European and Canadian scientists, supported by JAXA and ESA, decided to join forces and have proposed the EarthCARE mission described in this report.

NASA and its partners have planned two demonstrator missions. CloudSat (joint NASA – CSA mission) is a cloud profiling radar mission. It is planned to fly in formation with CALIPSO and EOS-AQUA. Currently, the CloudSat and CALIPSO are scheduled for a joint launch in spring 2005. CloudSat will fly a single instrument, a 94 GHz radar, the first cloud radar in space. The measurements are planned until the year 2008. The most important differences between CloudSat and the proposed EarthCARE radar are:

- The EarthCARE radar is almost 10 times more sensitive because of the larger antenna and lower orbit, and so will detect a higher percentage of radiatively significant clouds.

- The EarthCARE radar will have additional Doppler capability with resolution of up to 0.2 ms^{-1} so that it can detect convective motions (including those penetrating the tropopause) and the sedimentation velocities of ice particles in cirrus clouds, and derive more accurate drizzle rainfall rates.

The CALIPSO lidar satellite (joint NASA - CNES mission) is expected to be launched in spring 2005 into a nearly polar orbit, flying in formation with the CloudSat and EOS-AQUA satellites. The CALIPSO satellite will have two instruments: an imager and a lidar. The basic specification of the CALIPSO lidar is comparable to the one for EarthCARE with respect to the main backscatter and depolarisation capability, but will not have the High Spectral Resolution capability. The HSR lidar on EarthCARE will separate the Rayleigh (molecular) and Mie (cloud and aerosol) returns and so enable:

- Determination of the optical depth of aerosol in the boundary layer.

- Retrieval of independent profiles of extinction and backscatter, and hence profiles of their ratio, providing profiles of aerosol and ice crystal properties.

To accurately derive cloud microphysical parameters, measurements with lidar and radar have to be combined (Section 5.5). Because of the cloud variability at scales above 1 km, it is crucial that the lidar and radar observations are collocated. This is an inherent problem for the CloudSat and CALIPSO missions as the lidar and radar will be flying on separate platforms. Although the average across-track distance between the two platforms is predicted to be fairly small (better than 2 km), this can still introduce errors on the radar-lidar retrievals. Extensive simulations have shown that these errors in retrieved effective particle size and ice water content can be very large even with spatial separations of the order of 2 km. One of the problems is that it is very difficult to estimate the actual accuracy of the retrieved parameters in these cases.

CloudSat and CALIPSO should provide the first vertically resolved data set for cloud research and they should be an excellent test bed for EarthCARE algorithms and processing. Members of the EarthCARE science team are closely involved in the science teams of both CloudSat and CALIPSO. However, as noted above, there are fundamental differences between these missions and the more advanced instruments are on EarthCARE.

In addition, the Global Precipitation Measurement (GPM) mission, which continues the TRMM (Tropical Rainfall Measuring Mission), is planned and will have an additional 35 GHz radar to complement the single 14 GHz radar on the current TRMM. The major aim is to exploit the differential attenuation to provide more accurate rainfall estimates. The 35 GHz radar will only detect very dense clouds because its sensitivity is 40 dB less than with EarthCARE.

8.2 Contribution to International Programmes

The mission supports the goals of the World Climate Research Programme (WCRP), particularly its sub-programme Global Energy and Water Experiment (GEWEX), which aims to improve understanding of energy and water fluxes within the climate system, thereby securing reliable forecasts of weather and climate. This would enable a rather detailed description of the conversion of energy within the Earth's atmosphere. EarthCARE will also contribute to other WCRP programmes like SPARC. The atmospheric chemistry user community could use cloud and aerosol observations in their models, giving new insights into physical/chemical couplings in the atmosphere.

A well-defined strategy of inter-linked research activities will be beneficial to extend the objectives of EarthCARE. Central to this strategy is the bringing together of satellite observations, both operational (e.g. NPOESS, MetOp,) and experimental (Envisat, EOS). Efforts have already started to integrate experimental or research satellites following the recent WMO decision to consider such satellites as elements of the new Global Observing System (GOS), which is presently being implemented.

9. Application Potential

Apart from the various applications that stem directly from the mission objectives and are described in the previous chapters, EarthCARE measurements have great potential for further applications in different fields and for different purposes. This section provides an overview of the future potential uses of single EarthCARE instruments, as well as of the unique combination of active and passive sensors onboard the satellite.

9.1 Potential of Individual Elements

Various user communities might be able to use the observations from the four individual mission elements in their own particular fields. The land surfaces community could be served by providing conventional products like normalised differential vegetation index (NDVI), as the MSI is rather similar to AVHRR or other imagers. Similar to ICESAT, the lidar might be used for sea-ice detection. This might even become an operational application for use in, for example, polar ship navigation. Here also, the radar and the MSI could prove useful for providing cloud information. Observations using the radar might provide soil moisture information as the penetration depth would be of the order of 10 cm. Measurements of 94 GHz brightness temperature, i.e. using the receiver in a radiometer mode, might provide surface emissivity or temperature information. The BBR, with its forward and backward scanning capability will provide observations to continue and extend the Earth radiation budget data sets begun with ERB, CERES and ScaRaB.

Global statistics from the active instruments data could provide a wealth of information. Global lidar data from space, which started with LITE, are presently being complemented by data from ICESAT, and will in the future also be added to CALIPSO and ADM-Aeolus, can provide long term science data sets containing information about cloud, aerosol (sources and sinks) and pollution. The unique capability of the EarthCARE lidar to discriminate between different types of aerosols is of particular importance in this context. The lidar receiver could also be used for measuring surface properties in the near-ultraviolet.

9.2 Potential of Synergetic Use of Elements

Though the individual instruments can already provide a treasure trove in terms of observations for a variety of spin-off products, combining observations from mission elements on a single platform is the real strength EarthCARE. No other mission can provide anything similar in terms of synergy of active and passive instruments. EarthCARE will provide unique observations for the validation of a variety of ground-based networks.

The mission can serve the land surfaces user community with combined radar and lidar observations for improved surface characterisation. The release of aerosols by

pollution, biomass burning or volcano eruptions can be studied in detail using observations from the lidar and MSI combination. Such a data set can either complement ground-based or become the basis for global climatologies. Synchronised and co-located lidar, radar and multispectral imaging will be of a unique value for global climatologies of cloud and aerosol.

Beyond these potential application areas, the mission can also contribute to GMES, the European initiative for Global Monitoring for Environment and Security. Here the relevant topics will include land cover change and environmental stress in Europe, global vegetation monitoring (e. g. NDVI), and global atmosphere monitoring (aerosols, clouds, UV radiation, pollutants).

9.3   Potential for Operational Mission

As explained in Section 7, not only the climate modelling but also the numerical weather prediction community is actively preparing for the use of EarthCARE observations. This would imply that, if the mission is given the go-ahead, there might be an operational follow-up mission. This could have a similar basis or, using the experience gained with Cloudsat/CALIPSO and EarthCARE and possibly other missions, be related to, for example, precipitation, with a slightly different payload composition.

References

Ansmann A.J. et al., 2003: Long-range transport of Saharan dust to northern Europe: The 11-16 October 2001 outbreak observed with EARLINET, *J. Geophys Res.*, 108, 4783, doi:10.1029/2003JD003757.

Austin R.T., and G.L. Stephens, 2001: Retrieval of stratus cloud microphysical parameters using millimeter-wave radar and visible optical depth in preparation for CloudSat: 1. Algorithm formulation, *J. Geophys. Res.*, 106, 28,233-28,242.

Cooper S.J., T.S. l'Ecuyet and G.L. Stephens, 2003: The impact of explicit cloud boundary information on ice cloud microphysical property retrievals from infrared radiances, *J. Geophys. Res.*, 108, 4107-4123.

Cusack, S., Slingo, A., Edwards, J.M. and Wild, M., 1998: The radiative impact of a simple aerosol climatology on the Hadley Centre atmospheric GCM. *Q. J. R. Meteorol. Soc.*, 124, 2517-2526.

Donovan D.P., 2003: Ice cloud effective size parameterization based on combined lidar, radar reflectivity, and mean Doppler velocity measurements, *J. Geophys. Res.*, 108, 4573-4591.

Donovan, D.P., A.C.A.P. Van Lammeren, R.J. Hogan, H.W,J. Russchenberg, A. Apituley, P. Francis, J. Testud, J. Pelon, M. Quante, and J. Goddard, 2001: Cloud effective particle size and water content profile retrievals using combined lidar and radar observations, Part 2: Comparison with IR radiometer and in situ measurements of ice clouds, *J. Geophys. Res.*, 106, 27,449-27,464.

Duvel, J.P., M. Viollier, P. Raberanto, R. Kandel, M. Haeffelin, L.A. Pakhomov, V.A. Golovko, J. Mueller, R. Stuhlmann, and the International ScaRaB Scientific Working Group (ISSWG), 2001: The ScaRaB-Results Earth Radiation Budget Dataset and first results, *Bull. Amer. Meteor. Soc.*, 82, 1397-1408.

L'Ecuyer, T.S. and G.L. Stephens, 2003: The tropical oceanic energy budget from the TRMM perspective. Part I: algorithm and uncertainties, *J. Climate*, 16, 1967-1985.

European Space Agency, 1998: The Science and Research Elements of ESA's Living Planet Programme, ESA SP-1227, 105pp.

European Space Agency, 2001: Reports for Assessment, EarthCARE – Earth Clouds, Aerosols and Radiation Explorer; ESA SP-1257(1), 130pp.

Gettelman A., Salby M.L. and Sassi F., 2002: Distribution and influence of convection in the tropical tropopause region. *J. Geophys. Res.*, 107, 4080.

Higurashi, A., and T. Nakajima, 1999: Development of a two channel aerosol retrieval algorithm on global scale using NOAA / AVHRR. *J. Atmos. Sci.*, 56, 924-941.

Hogan R.J., M.D. Behera, E. O'Connor and A.J. Illingworth, 2004: Estimate of the global distribution of stratiform supercooled liquid water clouds using the LITE lidar. Accepted for publication in *Geophys. Res. Lett.*

IPCC (Intergovernmental Panel on Climate Change), 2001: Third Assessment Report, WG I Climate Change 2001: The Scientific Basis, Summary for Policy Makers.

Katagiri, S, and T. Nakajima, 2004: Radiative characteristics of cirrus clouds as retrieved from AVHRR, *J. Met. Soc. of Japan*, 82, in press.

Kaufman, Y.J., L. Remer, M. Chin, B.N. Holben, and D. Tanre, 2003: The global aerosol system and its direct forcing of climate: results from MODIS, AERONET and GOCART, IUGG Meeting, Sapporo, Japan.

Kawamoto, K., T. Nakajima, and T.Y. Nakajima, 2001: A global determination of cloud microphysics with AVHRR remote sensing. *J. Climate*, 14, 2054-2068.

Kristjánsson, J.E., J.M. Edwards, and D.L. Mitchell, 2000: Impact of a new scheme for optical properties of ice crystals on climates of two GCMs. *J. Geophys. Res.*, 105, 10063-10079.

Mattis I., A. Ansmann, U. Wandinger, and D. Müller, 2003: Unexpectedly high aerosol load in the free troposphere over central Europe in spring/summer 2003, *Geophys. Res. Lett.*, 30, 2178, doi:10.1029/2003GL018442.

Nakajima, T. and M.D. King, 1990: Determination of the optical thickness and effective particle radius of clouds from reflected solar radiation measurements. 1. Theory. *J. Atmos. Sci.*, 47, 1878-1893.

Nakajima, T., A. Higurashi, K. Kawamoto, J. Penner, 2001: A possible correlation between satellite-derived cloud an aerosol microphysical parameters, *Geophys. Res. Lett.*, 28, 1171-1174.

O'Connor, E.J., A.J. Illingworth and R.J. Hogan, 2004: A technique for auto-calibration of cloud lidar: In press: *J. Atmos. Oceanic. Technol.*

Okamoto H., S. Iwasaki, M. Yasui, H. Horie, H. Kuroiwa, and H. Kumagai, 2003: An algorithm for retrieval of cloud microphysics using 95-GHz cloud radar and lidar, *J. Geophys. Res.*, 108 4226- 4246.

Potter, G.L., and R.D. Cess, 2004: Testing the impact of clouds on the radiation budgets of 19 atmospheric general circulation models, *J. Geophys. Res.*, 109, D02106, doi:10.1029/2003JD004018.

Ramanathan, V., B.R. Barkstrom, and E.F. Harrison. 1989: Climate and the Earth's radiation budget. *Physics Today*, 42, 22-32.

Randall D., M. Khairoutdinov, A. Arakawa, and W. Grabowski (2003): Breaking the Cloud Parameterization Deadlock, *Bull. Amer. Meteor. Soc.*, 84, 1547–1564.

Reichardt J., S. Reichardt, A. Behrendt, and T.J. McGee, 2002: Correlations among the optical properties of cirrus-cloud particles: Implications for spaceborne remote sensing, *Geophys. Res. Lett.*, 29, doi:10.1029/2002GL014836.

Sekiguchi, M., T. Nakajima, K. Suzuki, K. Kawamoto, A. Higurashi, D. Rosenfeld, I. Sano, and S. Mukai, 2003: A study of the direct and indirect effects of aerosols using global satellite data sets of aerosol and cloud parameters, *J. Geophys. Res.*, 108, 4699, doi:10.1029/2002JD003359.

Slingo, A., 1990: Sensitivity of the Earth's radiation budget to changes in low clouds. *Nature*, 343, 49-51.

Takemura, T., 2003a: personal communication.

Takemura, T., 2003b: personal communication.

Takemura, T., T. Nakajima, O. Dubovik, B.N. Holben, and S. Kinne, 2002: Single scattering albedo and radiative forcing of various aerosol species with a global three-dimensional model, J. *Climate*, 15, 333-353.

Tinel, C., 2002: Restitution des propriétés microphysiques et radiatives des nuages froids et mixtes à partir des données du système RALI (radar/lidar), Phd. Thesis, Université Paris 7.

Wielicki, B.A., B.R. Barkstrom, E.F. Harrison, R.B. Lee III, G.L. Smith and J.E. Cooper 1996: Clouds and the Earth's radiant energy system (CERES): an Earth Observing System experiment. *Bull. Amer. Meteor. Soc.*, 77, 853-868.

Acronyms

ABC	Asian Brown Cloud
ACE	Arctic Cloud Experiment
AERONET	AErosol RObotic NETwork
AMIP	Atmospheric Model Intercomparison Project
ARM	Atmospheric Radiation Measurement
APEX	Atmospheric Particulate Environment Change Studies
ASTEX	Atlantic Stratocumulus Transition Experiment
AVHRR	Advanced Very High Resolution Radiometer
BALTEX	Baltic Sea Experiment
BBR	Broad Band Radiometer
BRDF	Bidirectional Reflectance Distribution Function
CALIPSO	Cloud-Aerosol Lidar and Infrared Pathfinder Satellite Observations
CAPT	CCPP-ARM Parameterization Testbed
CCPP	Climate Change Prediction Program
CERES	Clouds and the Earth's Radiation Energy System
ECMWF	European Centre for Medium-Range Weather Forecasts
ERBE	Earth Radiation Budget Experiment
EOS	Earth Observing System
GAW	Global Atmosphere Watch
GCM	General Circulation Model
GEWEX	Global Energy and Water Cycle Experiment
GMES	Global Monitoring for Environment and Security
GOS	Global Observing System
HSR	High-Spectral Resolution
INDOEX	Indian Ocean Experiment
IPCC	Intergovernmental Panel on Climate Change
IR	Infrared
ISCCP	International Satellite Cloud Climatology Project
IWC	Ice Water Content
JAMSTEC	Japan Marine Science and Technology Center
LITE	Lidar In orbit Experiment
LW	Longwave
LWC	Liquid Water Content
MERIS	Medium Resolution Imaging Spectrometer
MISR	Multi-angle Imaging SpectroRadiometer
MSI	Multi-Spectral Imager
NDVI	Normalised Differential Vegetation Index
NPOESS	National Polar-orbiting Operational Environmental Satellite System
NWP	Numerical Weather Prediction
PDF	Probability Distribution Function
POLDER	Earth Radiation Budget Scanning Radiometer
RMS	Root Mean Square

ScaRaB	Scanner for Radiation Budget
SKYNET	Network of surface sky radiation observation stations
SPARC	Stratospheric Processes And their Role in Climate
SW	Shortwave
TOA	Top of the Atmosphere
VIS	Visible
WCRP	World Climate Research Programme
WMO	World Meteorological Organization